Nano Research

Open Access

Review Article

Electric-field manipulation of nanofriction in 2D materials

Yuanhao Xu[1], Shuang Li[2], Lanyue Cui[1], Weixiang Sun[1] ✉, and Daoai Wang[2,3] ✉

[1] *School of Materials Science and Engineering, Shandong University of Science and Technology, Qingdao 266590, China*
[2] *State Key Laboratory of Solid Lubrication, Lanzhou Institute of Chemical Physics, Chinese Academy of Sciences, Lanzhou 730000, China*
[3] *Center of Materials Science and Optoelectronics Engineering, University of Chinese Academy of Sciences, Beijing 100049, China*

Cite this article: *Nano Research*, **2026**, *19*, 94908406. https://doi.org/10.26599/NR.2026.94908406

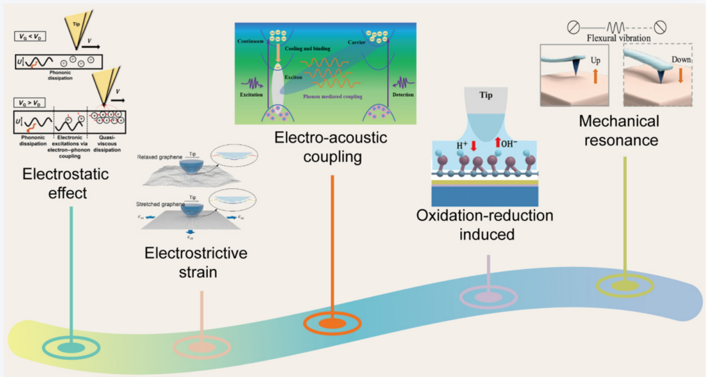

ABSTRACT: Two-dimensional (2D) materials have demonstrated immense potential in electronic devices, optoelectronic devices, and micro electro mechanical systems due to their unique structures and exceptional physicochemical properties. However, the tribological properties of 2D materials under carrier transportation conditions possess a significant impact on the reliability and lifespan of electronic devices, which poses a critical challenge for practical applications. Traditional macroscopic tribology theories are inadequate in explaining friction mechanisms at the nanoscale. Electric fields, as an effective control method, could dynamically regulate the interface friction behavior through various pathways such as carrier concentration, lattice strain, electron–phonon coupling, electric field-induced redox, and mechanical resonance. They have important potential in the fields of intelligent lubrication and friction sensing. However, the microscopic mechanism of friction energy dissipation under the action of electric fields is still unclear, especially the essence of the interaction between electrons and phonons. This review systematically reviews the modulation mechanisms of current-carrying friction in 2D materials, which includes electronic interactions, electrically induced strain, electron–phonon coupling, electric field-induced redox effects, and mechanical resonance. The relevant research indicates that applied electric fields could dynamically alter interfacial adhesion and energy dissipation pathways by modulating carrier concentration, lattice deformation, and surface chemical reactions. This capability enables precise control over friction coefficients. Furthermore, environmental factors (humidity) and multi-physical field coupling (electric and magnetic fields) exert additional influences on frictional behavior. This review exhibits the application potential of these mechanisms in low-power devices and intelligent lubrication systems. Additionally, it underscores the necessity of integrating multi-scale simulations with experimental validation in future studies. These researches would deepen mechanistic understanding and facilitate the development of novel modulation strategies.

KEYWORDS: two-dimensional (2D) materials, nanofriction, electric-field, friction manipulation, friction mechanisms

1 Introduction

Since graphene was discovered in 2004 [1], two-dimensional (2D) materials have rapidly become the focus and frontier of research in condensed matter physics, materials science, and nanotechnology [2, 3]. The number of this variety of material is constantly increasing, which includes zero-bandgap semimetals like graphene, transition metal chalcogenides with semiconductor properties (e.g., MoS_2 and WSe_2), hexagonal boron nitride (h-BN) with a wide bandgap, and emerging multicomponent alloys (e.g., $NiPS_3$ and $FePS_3$), as well as superconductors (e.g., $NbSe_2$) [4–6]. These new materials demonstrate that 2D materials possess a rich “gene pool” characteristic [7, 8]. The diversity and tunability enable 2D materials to demonstrate broad application prospects in the new generation of high-performance fields, low-power electronic devices, efficient optoelectronic devices, quantum information devices, and miniature energy storage devices [9–11]. However, during the actual operation of devices, 2D materials inevitably undergo mechanical contact and relative sliding [12]. These results adversely affect device performance and lifespan in friction and

Received: November 20, 2025; **Revised:** December 31, 2025
Accepted: January 5, 2026

✉Address correspondence to Weixiang Sun, sunweixiang@sdust.edu.cn; Daoai Wang, wangda@licp.cas.cn

wear [13, 14]. The energy dissipation caused by friction converts into additional heat sources other than Joule heat, which intensifies local temperature rise [15–17]. Wear directly damages the integrity of the material and leads to a significant increase in contact resistance, signal distortion, and even complete failure of the device [1, 18–20]. Therefore, the study for the frictional behavior of 2D materials, especially their microscopic current-carrying friction characteristics, is crucial for the fundamental solution to the reliability issues of 2D material devices and the promotion of their industrial application [21–24].

Traditional frictional theories are mainly based on macroscopic continuum mechanics. However, the above theories are difficult to explain the friction behavior of 2D materials at the nanoscale [25, 26]. In recent years, with the advancement of nanoscale characterization techniques such as atomic force microscopy (AFM) and friction force microscopy (FFM), researchers could directly observe and measure the friction behavior of 2D materials at the microscopic scale to reveal a series of novel phenomena and mechanisms different from traditional frictional theories [27, 28]. For example, it has been shown that the friction coefficient of 2D materials is closely related to their layer number, which is due to that the friction coefficient of single-layer materials is typically higher than that of multi-layer materials [29–31]. Additionally, the friction behavior of 2D materials is also affected by factors such as the material of the substrate and the temperature and humidity of the working environment [32–34]. Under current-carrying conditions, the friction behavior of 2D materials is more complicated [35, 36]. The introduction of an electric field not only changes the electronic structure of the material but may also cause Joule heating, electrical migration, and other effects, which would influence the friction properties of the material [37–39]. For example, related reports showed that the friction coefficient of graphene significantly decreases in the presence of an electric field [40, 41]. This phenomenon may be due to the variation in the surface charge density of graphene induced by the electric field [42]. However, some studies also found that the electric field could cause the friction coefficient of certain 2D materials to increase, which even leads to material wear and failure [43, 44]. These studies demonstrate that the current-carrying friction is a complicated multi-physics field coupling process which involves mechanics, electricity, thermodynamics, and other fields [45–47].

The study of the microscopic current-carrying friction mechanism in 2D materials is essential for the development of high-performance and low-power devices [48–50]. For example, for 2D material transistors, the contact resistance between the channel material and metal electrode and the friction wear are the key factors which affect the device performance [51, 52]. By regulating the microscopic current-carrying friction characteristics of 2D materials, it is possible to effectively reduce contact resistance and improve device stability and reliability [53]. Moreover, in micro-electromechanical systems (MEMS) and nano-electromechanical systems (NEMS) based on 2D materials, the friction and wear are also important factors which affect the device performance and lifespan [54–56]. Therefore, the investigation into microscopic current-carrying friction characteristics in 2D materials is of paramount importance for enabling the practical application of 2D material devices [57–60].

Despite considerable research progress on microscopic current-carrying friction in 2D materials, multiple challenges continue to exist [61–63]. For instance, the underlying mechanism of current-carrying friction in 2D materials has yet to be fully elucidated [64, 65]. Consequently, the research community has yet to establish comprehensive theoretical models or a robust body of experimental evidence [66–68]. Moreover, effective control of the current-carrying friction properties in 2D materials to meet the requirements of different application scenarios remains an urgent challenge [69–71]. In the future, it is essential to integrate experiments, theories, and simulations to conduct in-depth investigations into the microscopic current-carrying friction mechanisms of 2D materials [72–74]. Furthermore, novel material designs and surface modification approaches should be explored to achieve precise regulation of the current-carrying friction properties in such materials [75, 76].

Therefore, this review aims to systematically summarize recent advances in the field of microscopic current-carrying friction of 2D materials [83]. It focuses on elucidating the mechanisms, through which applied electric fields or currents modulate frictional behavior via various pathways, such as electron interactions, electrostriction, electron–phonon coupling, redox effects, and mechanical resonance (Fig. 1). This review examines the influence of environmental factors and multi-physical field coupling, explores the application potential in related devices, and outlines key challenges along with future research directions [84, 85]. By deepening the understanding of the microscopic current-carrying friction mechanism, it is expected to provide a solid scientific foundation for designing reliable, high-performance, and intelligent 2D material devices [86–89]. This would accelerate the transformation process of 2D material microscopic tribology from basic research to practical application [90, 91].

2 The microscopic carrier transport mechanism of 2D materials

2.1 Electrostatic effect

In the microscopic friction process of 2D materials, the variations in electrostatic force caused by the accumulation and dissipation of charges are one of the main influencing factors [92]. Based on macroscopic tribology research, it has been shown that when two different materials come into contact and rub against each other, electrons would transfer from a surface that is more prone to losing electrons to another surface [93–95]. The transfer of electrons leads to the accumulation of electric charge, and this phenomenon is caused by the difference in electron affinity. At this moment, these two frictional surfaces carry opposite charges respectively, and the accumulation of these opposite charges generates electrostatic force, which causes them to attract each other [96]. Through extensive existing studies, it has been shown that this mechanism of electrostatic force action is also applicable in the microscopic friction behavior of 2D materials [97, 98]. However, when an external electric field is applied, the external electric field would change the electrostatic force between the friction pairs and the friction behavior [99–101].

Yu et al. (2020) studied the nanoscale friction characteristics of h-BN under the induced electrostatic interaction of an electric field [76]. By sliding the conductive AFM probe on the surface of h-BN, the authors measured the friction force and adhesion force of h-BN under different substrate bias voltages. As the bias voltage difference between the probe and the substrate increased, the nanoscale friction force of h-BN significantly increased. Besides, the friction

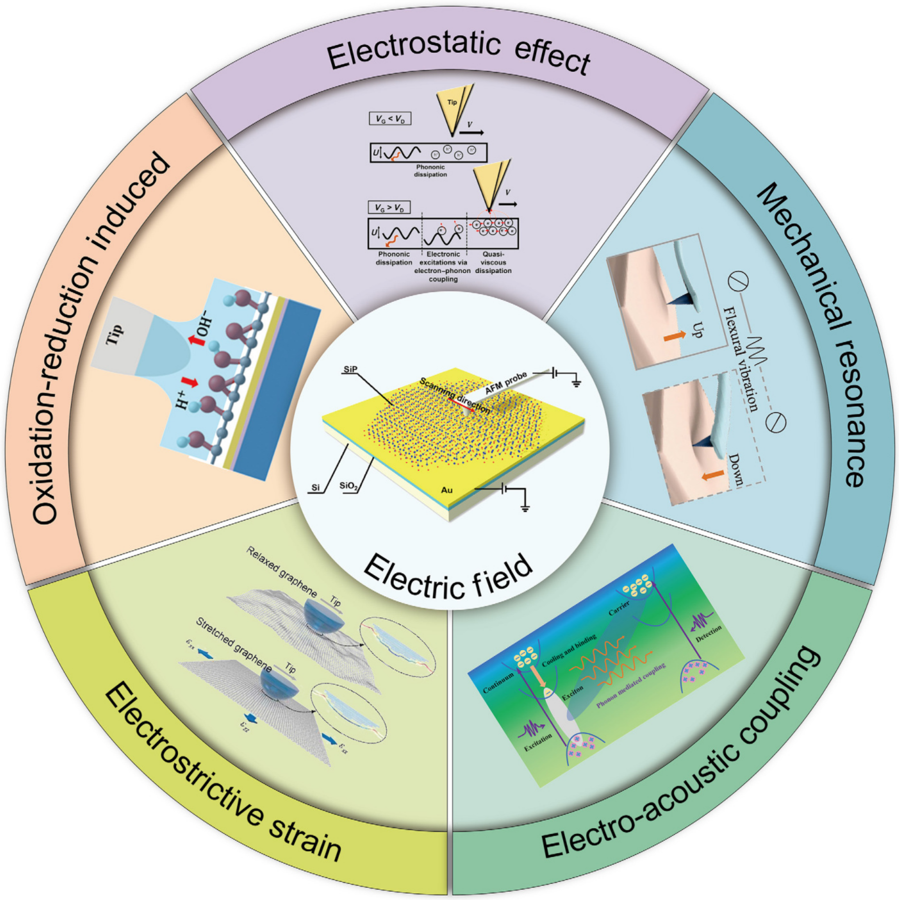

Figure 1 The mainstream friction mechanism under the influence of an external electric field [77–82]. Reproduced with permission from Ref. [77], © 2019. Published under the PNAS license; Ref. [78], © Cao, J. W. et al. 2021; Ref. [79], © Greenwood, G. et al. 2023; Ref. [80], © American Chemical Society 2021; Ref. [81], © Elsevier Ltd. 2025; Ref. [82], © American Chemical Society 2023.

force under negative bias was greater than that under positive bias and the friction force returned to its original size when the bias was removed (Fig. 2(a)). This variation in friction force is closely related to electrostatic interaction, and the increase in electrostatic force would change the contact area between the probe and h-BN, which could affect the friction force. Although the study by Yu et al. demonstrated how an external field can enhance friction through electrostatic attraction, subsequent research revealed that electric fields can also be harnessed to dramatically reduce friction, depending on the material system and interface conditions. Shi et al. (2021) studied the friction behavior of MoS_2 under the action of an electric field [102]. By rubbing the MoS_2 surface under an electric field condition and then removing the external electric field for scanning MoS_2 over a larger area, the authors found that the electric field could significantly reduce the friction coefficient of MoS_2 to an ultra-low friction state (with a friction coefficient of approximately 0.0045) (Fig. 2(b)). They proposed that the AFM tip and MoS_2 under the effect of the electric field led to the transfer and accumulation of charges at the interface between MoS_2 and SiO_2/Si substrate. And the electrostatic force between the charges enhanced the binding strength between MoS_2 and the substrate, which would suppress the atomic-scale deformation of MoS_2 surface and reduce the effects of wrinkling and local adhesion on friction to achieve ultra-low friction (Fig. 2(c)).

The concentration and distribution of charge carriers (electrons or holes) in 2D materials significantly affect their microscopic frictional properties [103]. By applying an external electric field to change the energy barrier for carrier migration and regulate the accumulation or dissipation of carriers, the surface charge density of 2D materials could be altered, thereby controlling the electrostatic force and adhesion force with the contact interface [43]. Enhanced electron–phonon coupling due to more charge carriers could cause greater energy dissipation and a corresponding increase in frictional force. This dual regulation effect of charge carriers on friction depends on the electronic properties of the material, the carrier mobility, and the interaction with the environment. Overall, the external electric field provides a flexible way to control the frictional properties of 2D materials and opens up novel directions for their application in intelligent friction regulation and micro-nano devices.

As early as 2006, Park et al. studied the effect of carrier concentration in the pn junction of silicon on nanoscale friction using conductive AFM (C-AFM) (Fig. 3(a)) [59, 104]. The study found that when a forward bias (+4 V) was applied to bring the p-region into a strong accumulation state, the friction force significantly increased (about 1.6 times higher than the n-region), while no significant difference was observed under reverse bias (−4 V) (Fig. 3(b)). By systematically changing the load, scanning speed, and needle tip passivation treatment, the authors excluded the influence of current-induced chemical effects, local heating, or wear, and confirmed that the increase in friction force was directly related to the accumulation of hole charge carriers. This work was

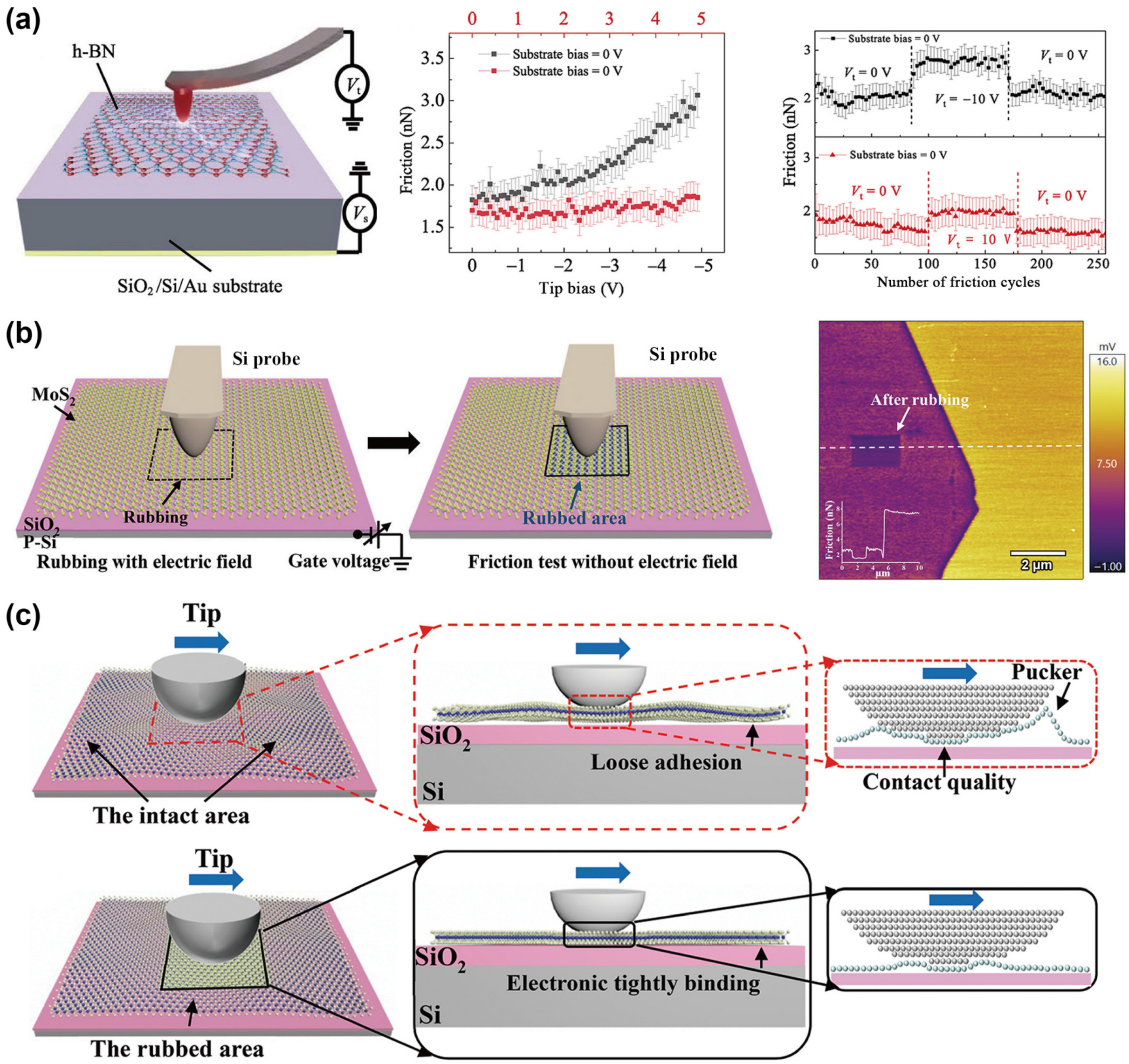

Figure 2 (a) Schematic diagram of the C-AFM experimental setup. The relationship between frictional force and the tip bias voltage. Reproduced with permission from Ref. [76], © Yu, K. M. et al. 2020. (b) Schematic diagram of the friction experiment and the friction force graph of MoS_2. (c) Schematic diagram of friction of MoS_2. Reproduced with permission from Ref. [102], © The Royal Society of Chemistry 2021.

the first to achieve active control of friction behavior through the electrical regulation of carrier concentration in a semiconductor system. It provided a prototype example for electronic friction control in micro-nano electromechanical systems. Shi et al. used gate voltage to regulate the carrier concentration of single-layer MoS_2 and systematically studied the contribution of carrier concentration to friction dissipation (Fig. 3(c)) [105]. Their experiments showed that the carrier concentration increased, and this enhanced the strength of the electron-phonon coupling, which in turn caused the friction force to increase linearly. This trend aligned with the theoretical prediction of the Langevin equation (Fig. 3(d)). Through the Raman spectroscopy and surface potential analysis, the authors confirmed the direct correlation between the softening of the A_{1g} acoustic mode and the carrier concentration (Fig. 3(e)), which reveals the dominant role of electron friction in energy dissipation.

In addition to the study of the material's own properties, the interaction phenomena between the material and different probes are also of great significance. Greenwood et al. (2023) studied the friction behavior between single-layer graphene and an AFM probe under the action of an external electric field (Fig. 4(a)) [79]. Through the use of graphene field-effect transistor (FET) devices, the authors regulated the carrier density of graphene in a dry nitrogen environment and measured the friction force and electrostatic interactions with different types of probes (insulating, conductive, and semiconductor probes). The study found that when graphene was in contact with a semiconductor probe, the friction exhibited significant enhancement and tunability (Fig. 4(c)), which was closely related to the charge density of graphene, and the variation in friction force was particularly obvious near the Dirac point of graphene. At the same time, the average amplitude of the stick slip appears to have a minimum at the Dirac point and slightly increases as the gate voltage moves away from V_D in either direction (Fig. 4(b)). The results showed that by electrically regulating the charge density of graphene, the dynamic control of friction could be achieved.

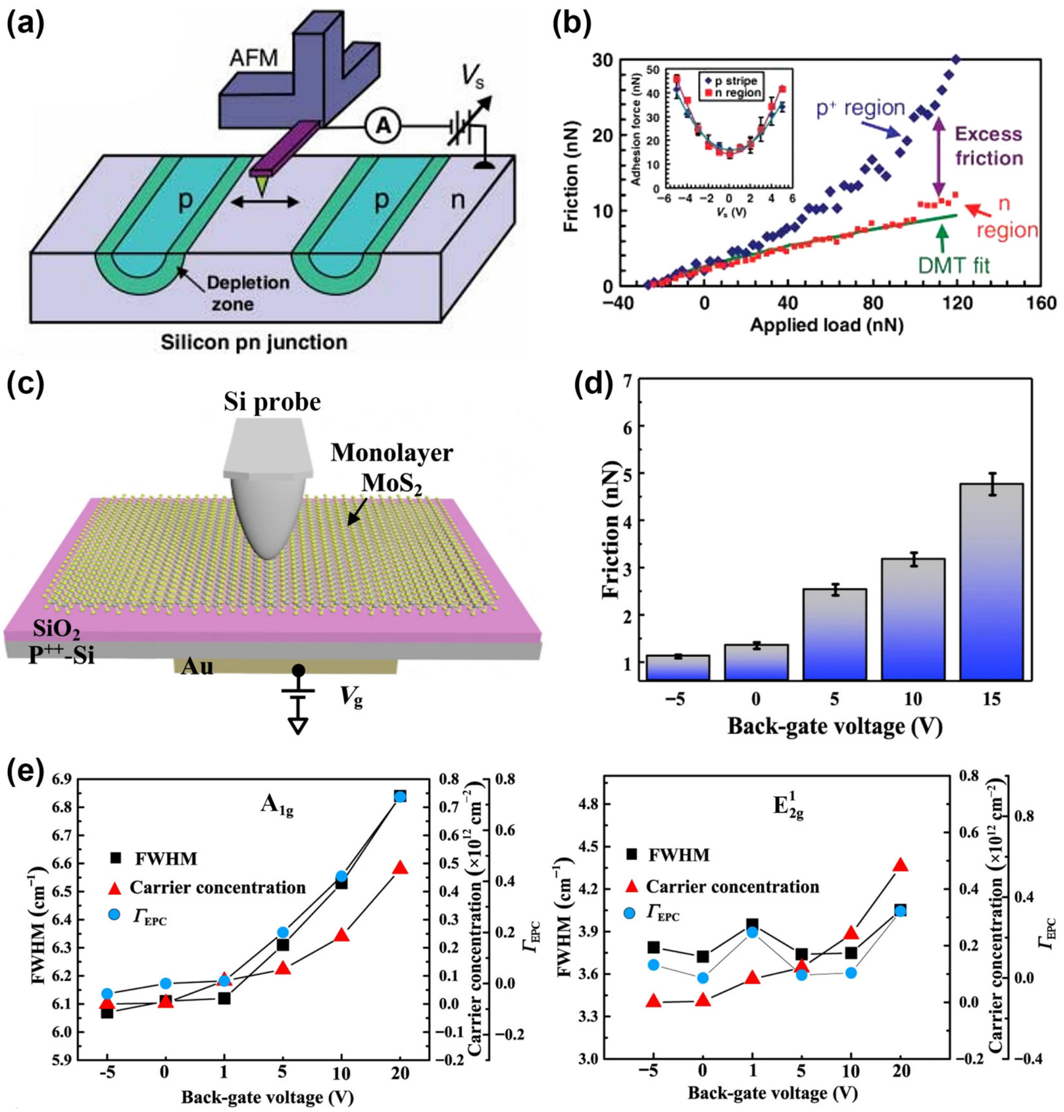

Figure 3 (a) Schematic of AFM measurements on a silicon pn junction devic. (b) Plot of friction force as a function of applied load at +4 V sample bias. Reproduced with permission from Ref. [59], © American Association for the Advancement of Science 2006. (c) Schematic of the nanofriction measurements on atomically thin MoS_2 under different V_g. (d) The nanofriction on atomically thin MoS_2 varied with the different V_g. (e) FWHM and carrier concentration of A_{1g} and E^1_{2g} mode as a function of V_g. Reproduced with permission from Ref. [105], © Shi, B. et al. 2022.

Under electric field conditions, the directional migration of charge carriers is often the result of a competition between the electric field, the material's own potential barrier, and frictional and flexural electric effects. Qiao et al. (2021) experimentally studied the coupling mechanism of frictional electric effect and flexural electric effect at the nanoscale [106], and demonstrated that the charge transfer is jointly determined by these two effects in the presence of a strain gradient. When the charge transfer directions of the frictional and flexural electric effects are the same, the charge transfer is enhanced; while when the directions are opposite, the direction and magnitude of charge transfer could be regulated by the variation in the normal force (Figs. 5(a) and 5(b)). The study also found that as the normal force increases, the flexural electric effect gradually becomes dominant and reverses the direction of charge transfer. Additionally, by applying a bias voltage on the AFM probe, the research team further verified the important role of the flexural electric effect in charge transfer (Fig. 5(c)).

Although the aforementioned mechanisms have revealed multiple ways in which the electric field regulates the frictional behavior of 2D materials, a full understanding of the underlying principles of these phenomena still requires a return to the fundamental energy transfer and dissipation principles in the friction process. Li et al. (2025) studied the friction behavior of single-layer MoS_2 under current-carrying conditions using the C-AFM and scanning Kelvin probe microscope (SKPM) system (Fig. 6(a)) [107]. They found that within the ±4 V bias range, the friction force under negative bias was significantly higher than that under positive bias (0.78 nN at −4 V and 0.084 nN at +4 V), and this difference increased with the increase in voltage (Figs. 6(b) and 6(c)). Through surface potential mapping and atomic-level friction imaging, the authors revealed that the mechanism originated from the asymmetric charge accumulation due to the inherent work function difference between the probe and MoS_2: Negative bias promoted the injection of a large number of electrons into the MoS_2 surface, while positive bias only caused limited charge transfer. Atomic-level sliding experiments further demonstrated

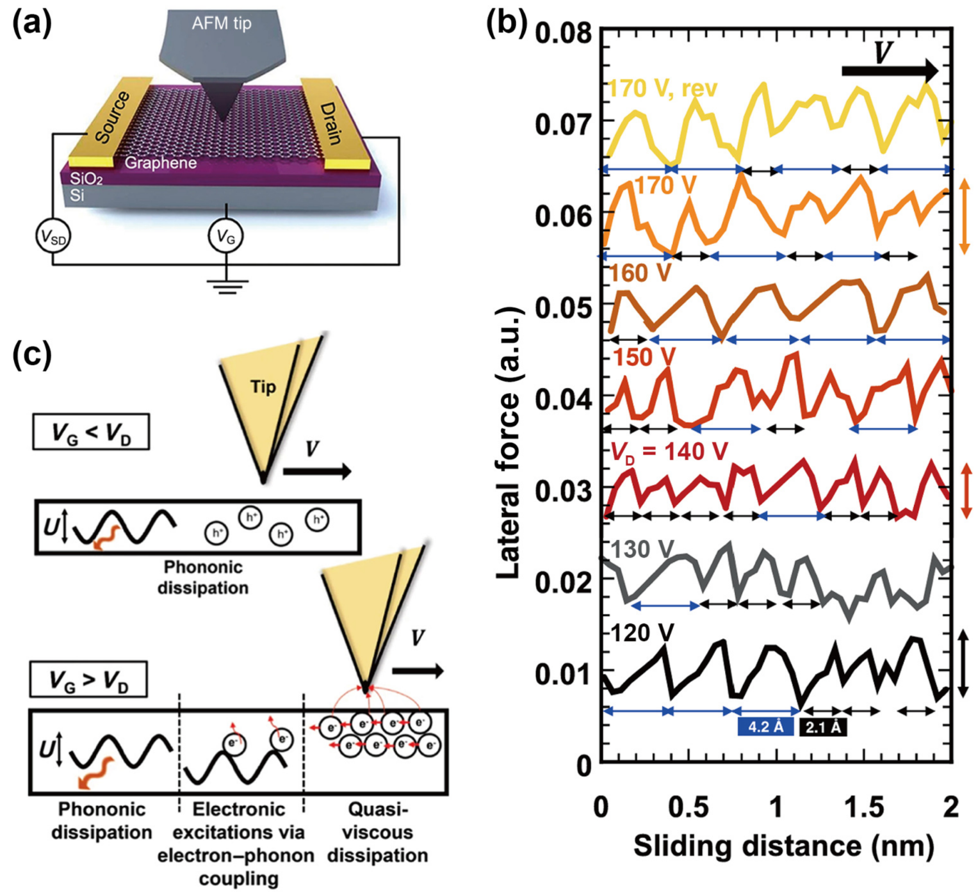

Figure 4 (a) Schematic illustration of *in situ* electrical characterization of graphene FETs during friction measurement. (b) Stick-slip behavior of a Si tip sliding on graphene at selected V_G values. (c) Schematic diagram of dissipation mechanism. Reproduced with permission from Ref. [79], © Greenwood, G. et al. 2023.

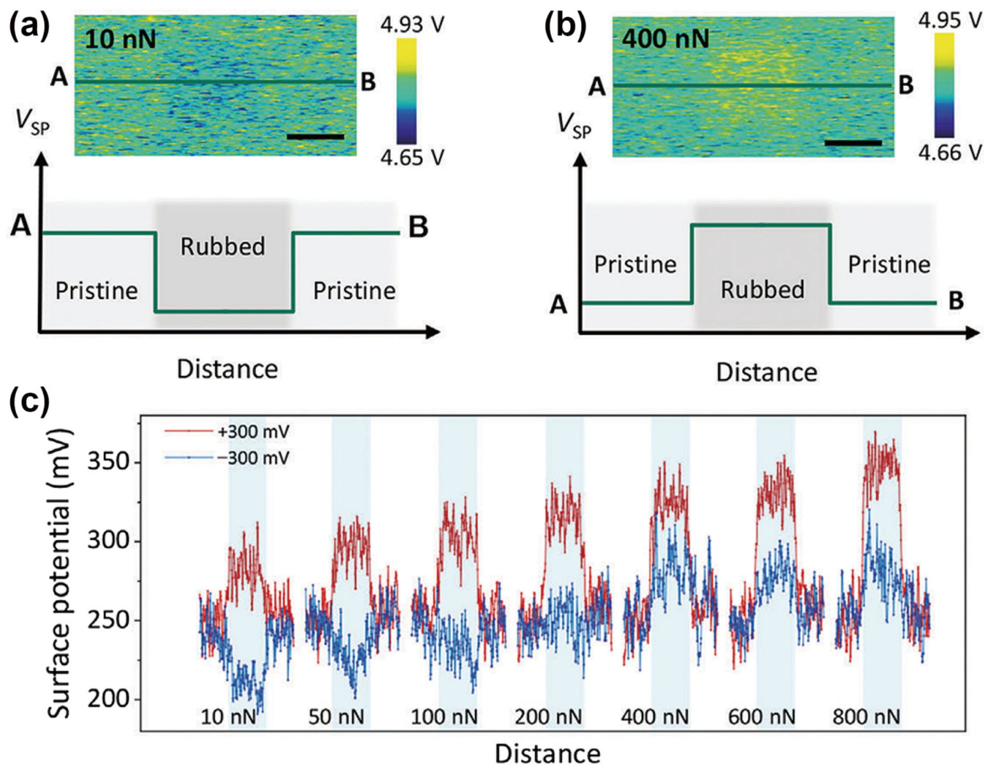

Figure 5 ((a) and (b)) Corresponding (top) representative work function images and (bottom) illustrative surface potential profile across rubbed region under low and high normal forces. (c) Under different normal forces, the surface potential distribution after friction. Reproduced with permission from Ref. [106], © Qiao, H. M. et al. 2021.

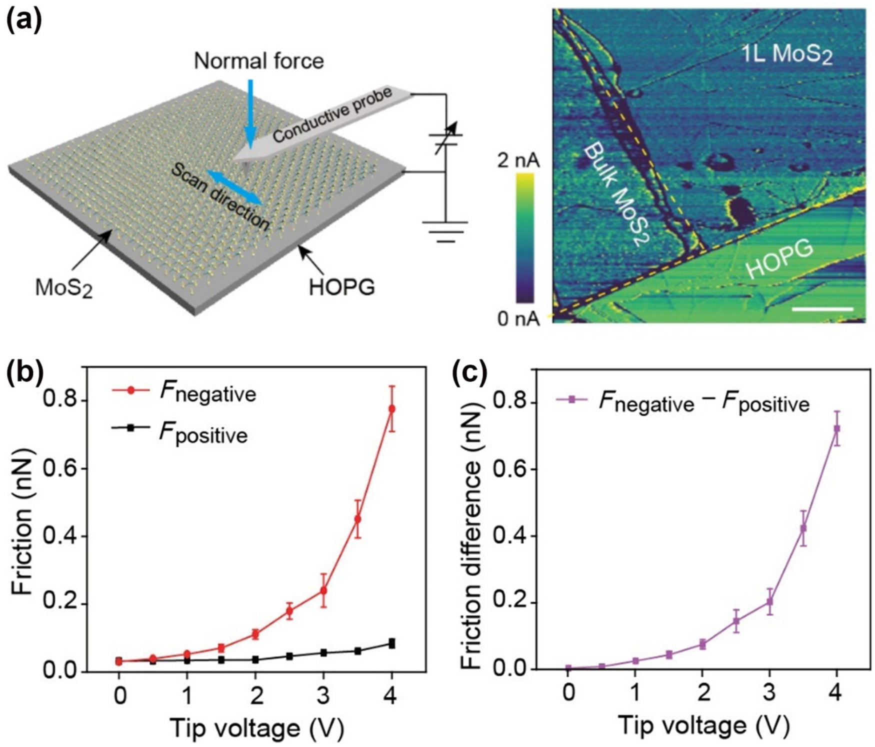

Figure 6 (a) Schematic illustration of the current-carrying friction experiment using conductive AFM, and current map of monolayer and bulk-like MoS_2 on HOPG substrate. (b) Friction force measured on monolayer MoS_2 at different positive and negative tip voltages. (c) Difference in friction force as a function of tip voltage. Reproduced with permission from Ref. [107], © Elsevier B.V. 2024.

that the negative bias increased the interface potential barrier by 40%, resulting in 2.3-fold increase in the single-cell energy dissipation at 0 V.

2.2 Electrostrictive strain

The surface strain of 2D materials has a significant impact on their friction characteristics. The strain could alter the local structure and electronic properties of the material, thereby affecting the interaction between its surface and the contacting object [108–110]. Generally, tensile strain usually enhances the stiffness and hardness of the material, thereby reducing the friction force; while compressive strain may cause the material to become softer, increasing the friction force [111]. The strain may also affect the surface roughness and adhesion force in the friction interface, further changing the friction characteristics. Under the action of an electric field, 2D materials may undergo surface shape deformation (such as undulation or bending) or lattice distortion due to changes in stress distribution caused by the electrostriction effect or ion migration, thereby changing their surface roughness and the actual contact area at the contact interface [112]. Such deformation may cause changes in the adhesion force and friction force at the contact interface, thereby reducing the friction force; while excessive deformation may lead to local stress concentration, increase friction, or cause interface wear [111]. Additionally, lattice deformation may affect the electronic structure of the material, thereby changing the electronic and phonon coupling mechanism during the friction process. These effects jointly determine the complicated evolution law of the microscopic friction characteristics. This understanding provides theoretical support for the application of these materials in nanoscale friction control and intelligent surface design.

He et al. (2019) studied the influence of the electric potential gradient in the plane on the friction behavior of 2D materials (MoS_2, graphene, and h-BN) through experiments and theoretical calculations [113]. The team found that when a lateral electric field was applied to MoS_2 using the plane electric potential gradient, the friction force on the MoS_2 surface significantly decreased, and the friction force further decreased with the increase of the electric potential gradient (Fig. 7(a)), and the same phenomenon occurred in graphene and h-BN. By analyzing the atomic-level sliding motion, they believed that applying the plane electric potential gradient changed the lattice shape of the 2D material, suppressed the high friction dissipation process, and thus achieved the reduction of the friction force (Fig. 7(b)).

Although the study by He et al. revealed the physical mechanism by which the planar electric potential gradient regulates the friction behavior of traditional two-dimensional material, indicating that the electric field can suppress frictional dissipation by altering the crystal lattice morphology of the materials, the potential of electric field regulation is far beyond these classic two-dimensional systems. In recent years, with the continuous emergence of new two-dimensional materials, researchers have begun to explore the regulatory effect of the electric field on the friction performance of more complex two-dimensional systems, especially two-dimensional metal-organic framework materials with porous structures and adjustable chemical properties, providing a new platform for understanding the coupling mechanism between the electric field and interface friction. In this context, Li et al. (2025) studied the super-lubrication characteristics and regulation mechanism of 2D zeolitic imidazolate framework-8 (ZIF-8) under the action of an electric field [114]. Through experiments and simulations, it was found that longitudinal and lateral electric fields

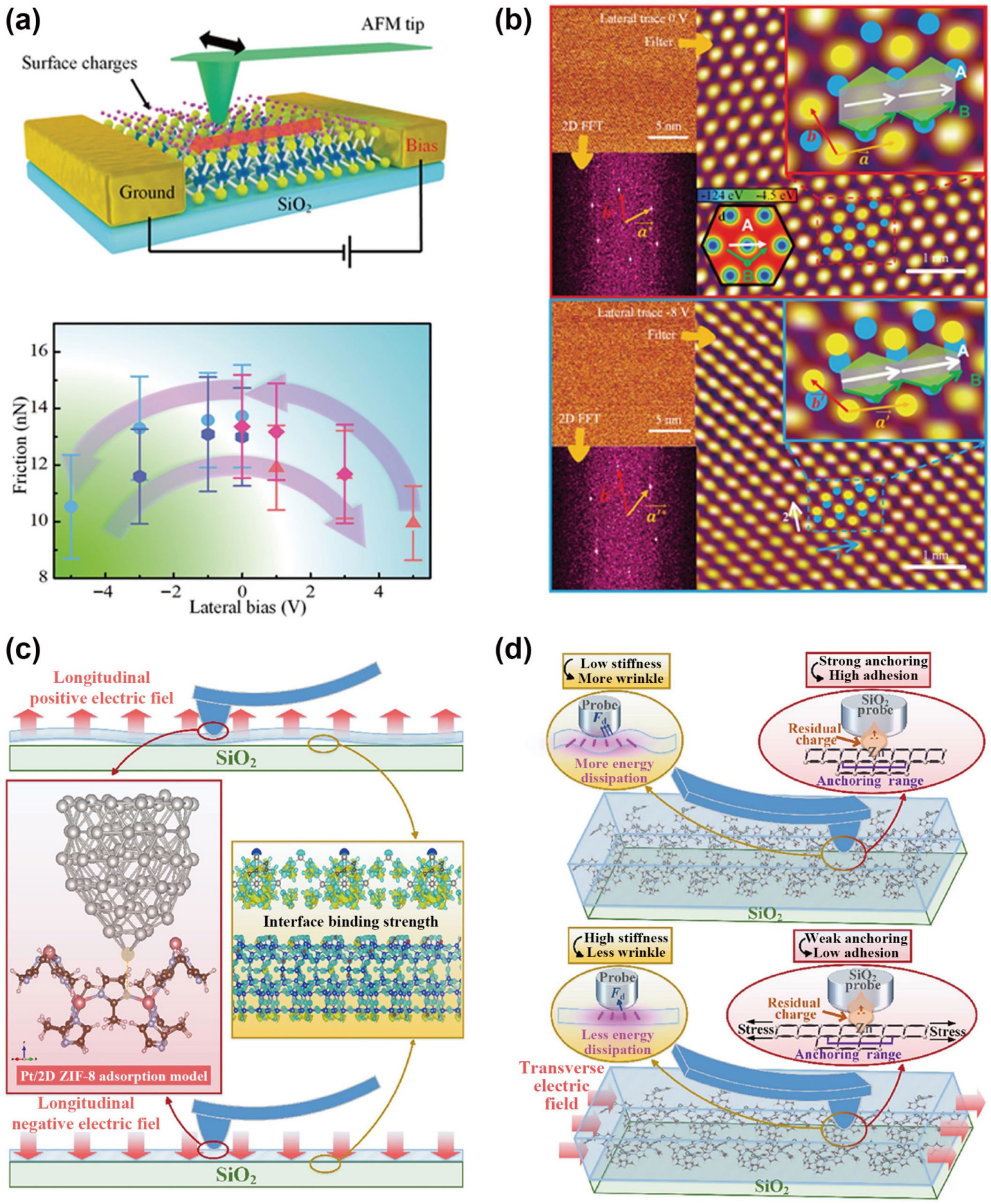

Figure 7 (a) Schematic diagram of the AFM friction experimen. Variations in the friction force with bias voltage. (b) Atomic-scale friction maps. Reproduced with permission from Ref. [113], © WILEY-VCH Verlag GmbH & Co. KGaA, Weinheim 2019. (c) The regulation mechanisms of 2D ZIF-8 surface superlubricity by longitudinal and (d) transverse electric fields. Reproduced with permission from Ref. [114], © Elsevier Ltd. 2024.

could significantly regulate the friction coefficient of ZIF-8. In the longitudinal electric field (Fig. 7(c)), the negative bias weakens the anchoring effect between the conductive probe and the surface of ZIF-8, reducing the interfacial adhesion force; at the same time, the redistribution of charge at the interface between ZIF-8 and SiO_2 substrate enhances the interface bonding strength, thereby suppressing the out-of-plane deformation during the sliding process and significantly reducing the friction. In the lateral electric field (Fig. 7(d)), both positive and negative biases could cause lattice stretching strain in ZIF-8, leading to the electron cloud shift of Zn–N coordination bonds and the reduction of surface residual charges, further reducing the adhesion force between the probe and ZIF-8. Additionally, lattice strain also enhances the surface stiffness of the material, reducing the energy dissipation during sliding. These findings reveal the dual mechanism of electric field regulation of ZIF-8 lubrication performance: the coupling effect of adhesion regulation and out-of-plane deformation regulation.

2.3 Electron–phonon coupling

2D materials exhibit significant surface–electron–phonon coupling effects due to their atomic-scale thickness and high surface-to-volume ratio [115–117]. The electron–phonon coupling refers to the influence of surface charges (electrons) on the energy dissipation and motion behavior of the material through their interaction with lattice vibrations (phonons) [118]. During friction, the relative sliding of the interface leads to the excitation of

Tsinghua University Press | SciOpen

phonons, and the coupling between phonons and surface charges alters the energy dissipation path, thereby regulating the magnitude of friction. Additionally, the electron–phonon coupling could enhance the local interaction between electrons and the lattice, which further affects the viscosity and sliding behavior of the contact interface. When an external electric field is applied, the electric field changes the distribution of surface charges on the 2D material, thereby affecting the strength of the electron–phonon coupling. Specifically, the applied electric field could induce the redistribution or doping of electrons, thereby altering the excitation characteristics of phonon modes and the efficiency of electron–phonon coupling. The direction and intensity of the electric field, along with the material's specific structure and properties, determine whether this effect increases or decreases the frictional force. Therefore, it is theoretically possible to control the frictional behavior of 2D materials dynamically by adjusting the applied electric field, and this offers new possibilities for the design of nano-devices and the regulation of friction.

In 2009, Filleter et al. studied the friction and dissipation characteristics of monolayer (1LG) and bilayer (2LG) graphene films grown epitaxially on SiC (Fig. 8(a)) [119]. They found that the monolayer graphene significantly reduced the friction of SiC, while the friction of the bilayer graphene was further reduced by approximately half (Fig. 8(b)). Through angle-resolved photoemission spectroscopy (ARPES), the authors revealed that this friction difference originated from the significant difference in electron–phonon coupling between the monolayer and bilayer graphene (Fig. 8(c)). Specifically, the electron–phonon coupling in the monolayer graphene was stronger, resulting in higher energy dissipation efficiency and increased friction. In contrast, the electron–phonon coupling in the bilayer graphene was weaker, leading to lower friction. The research by Filleter et al. on the graphene/SiC system demonstrated that the non-equilibrium dynamics of electron–phonon coupling is the core mechanism for regulating interface friction in the absence of carriers, providing important insights for understanding frictional regulation under carrier conditions.

Under electric field conditions, the influence of electron–phonon coupling on the nanoscale friction behavior of 2D materials is more pronounced. Sohier et al. studied the electron–phonon coupling behavior of graphene under the action of an electric field using density functional perturbation theory (DFPT) [120], particularly focusing on the coupling mechanism of bent phonons. They found that the electric field significantly alters the phonon spectrum of graphene and activates the coupling between bent phonons and electrons that was previously prohibited due to symmetry.

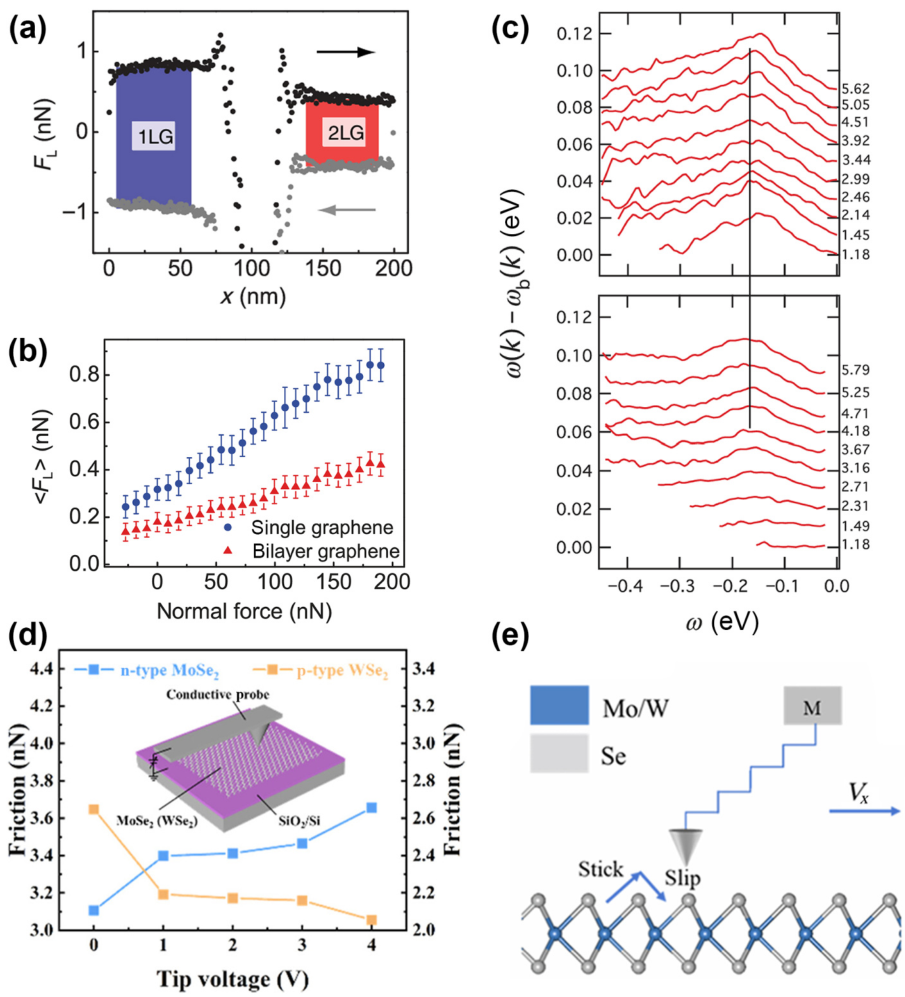

Figure 8 (a) Friction loop recorded on a boundary region of the sample. (b) Average lateral force of 1LG and 2LG. (c) Corresponding kink magnitude varies with the doping value. Reproduced with permission from Ref. [119], © The American Physical Society 2009. (d) Schematic of $MoSe_2$ and WSe_2 nanofriction measurement. (e) Schematic of the movement of AFM probes on the surfaces of $MoSe_2$ and WSe_2. Reproduced with permission from Ref. [121], © American Chemical Society 2025.

However, this coupling is strongly shielded in doped graphene, resulting in negligible contribution in the presence of carriers. Huang et al. (2025) synthesized single-layer n-type $MoSe_2$ and p-type WSe_2 using chemical vapor deposition (CVD) and systematically studied the carrier-type-dependent friction mechanism of 2D transition metal dichalcogenides (TMDs) under a positive electric field using atomic force microscopy [121]. The study found that with the application of a positive voltage (0–4 V), the friction force and friction coefficient of n-type $MoSe_2$ significantly increased (from 0.006 to 0.030), while p-type WSe_2 showed the opposite trend (from 0.033 to 0.012) (Fig. 8(d)). Through the surface potential (SKPM) and atomic-level sliding behavior analysis, it was revealed that carriers either accumulate (in n-type materials) or dissipate (in p-type materials) on the surface. This behavior regulates the surface potential. The electric field did not cause a significant change in the adhesion force of the material. This indicates that the variations in friction are mainly due to the energy dissipation caused by electron–phonon coupling (Fig. 8(e)).

Ohmic dissipation is one of the important manifestations of the electron–phonon coupling effect [122–124]. Due to the high mobility of electrons in 2D materials, when the material interface undergoes relative sliding, the energy dissipation (i.e., Ohmic dissipation) generated by the scattering of electrons would be converted into thermal energy [125], thereby affecting the magnitude of the interface friction [126, 127]. The Ohmic dissipation mechanism is closely related to the interface electron–phonon coupling and carrier scattering, and determines the conversion path of frictional energy. Under an applied electric field, the electric field regulates the carrier density and electron transition behavior in 2D materials, thereby changing the strength of electron–phonon coupling and the efficiency of Ohmic dissipation [128–130]. When an external electric field is applied to 2D materials, electrons within the material and at the interface would move directionally under the drive of the electric field, forming an electric current [131–133]. This charge movement triggers the Ohmic dissipation through the electron–phonon scattering, that is, some electrical energy is converted into thermal energy, thereby increasing the energy dissipation at the interface. Since the energy dissipation directly affects the magnitude of friction and the sliding behavior, the Ohmic dissipation effect leads to an increase in frictional force. Additionally, the external electric field may also change the conductivity of the material and the local charge distribution, further regulating the variations in frictional force [134, 135].

Wang et al. (2025) prepared single-layer $NbSe_2$ films using CVD method (Fig. 9(a)) and studied the regulation mechanism of bias electric field on the friction behavior of 2D $NbSe_2$ using a C-AFM system (Fig. 9(b)) [136]. The experiment found that in the ±1.5 V bias voltage range, the friction force and friction coefficient of $NbSe_2$ both significantly increased with the increase in voltage (the friction coefficient increased from 0.024 to 0.085 under positive bias, and from 0.024 to 0.058 under negative bias) (Figs. 9(c) and 9(d)), and the regulation effect of positive bias was stronger. Through force–distance curves and surface potential (SKPM) measurements, it was revealed that this asymmetry originated from the difference in electrostatic adsorption caused by the inherent potential difference between the probe and $NbSe_2$: Positive bias made the electrostatic adsorption force follow the quadratic growth

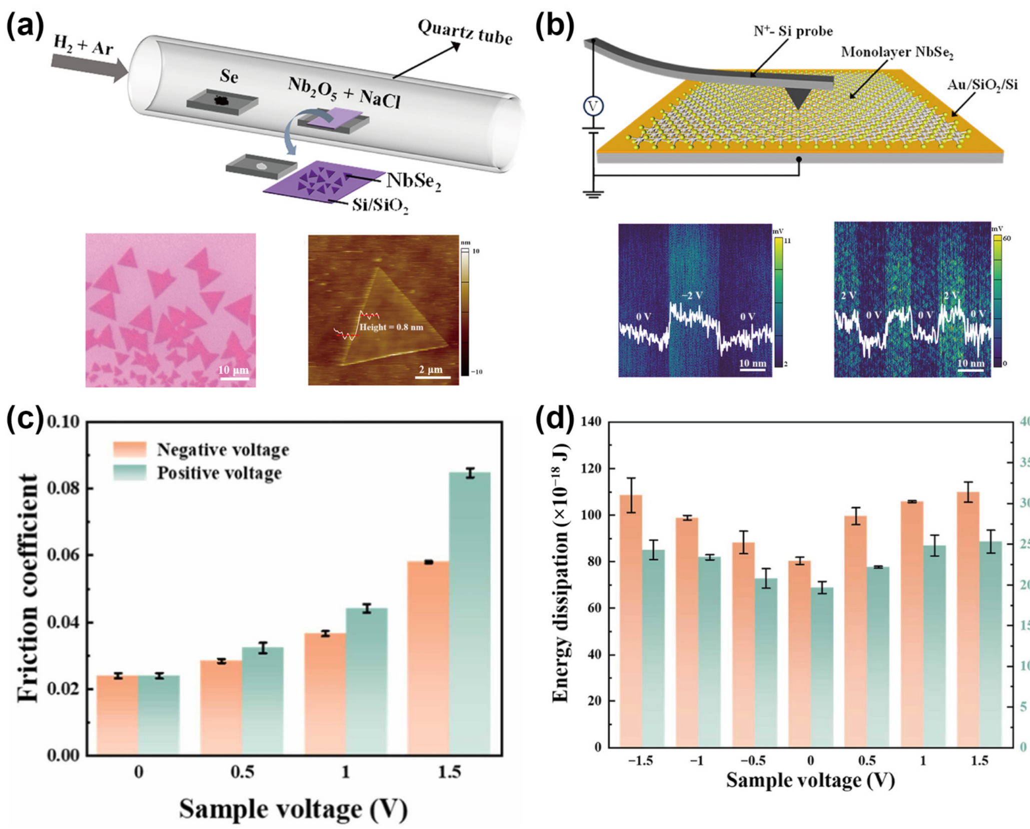

Figure 9 (a) Preparation and characterization of $NbSe_2$. (b) Nanofriction measurement diagrams under different normal bias. (c) Adhesive force values under different bias, highlighting differences between positive and negative bias. (d) Energy dissipation and maximum lateral peak force under different bias. Reproduced with permission from Ref. [136], © Elsevier Ltd. 2025.

of $F_{aa} = 0.92(V + 0.07)^2 + 24.68$, while the negative bias partially neutralized the inherent potential difference. Atomic-level sliding experiments further indicated that the electric field-induced carrier excitation was converted into local thermal dissipation through the electron–phonon coupling, enhancing the energy dissipation with the increase in bias voltage. This study established for the first time a complete correlation model of "electric field–carrier excitation–energy dissipation–friction" in $NbSe_2$.

2.4 Oxidation–reduction induced by electric field

The oxidation–reduction of the surface of 2D materials induced by an electric field significantly affects their microscopic friction properties. Variations in the chemical state of the surface of 2D materials, such as modification of surface functional groups, chemical doping, or oxidation, also alter the electronic structure and surface energy of the material, thereby affecting the adhesion force and sliding resistance at the interface [137–139]. When an electric field acts on 2D materials, their surfaces chemically react with oxygen or water molecules from the environment. This reaction leads to the formation of oxides or the incorporation of functional groups such as hydroxyl or carboxyl groups. As a result, the chemical composition and physical properties of the surface are altered. This surface modification increases the surface energy and polarity of the material. This enhances the adhesion force and shear strength at the contact interface and causes an increase in the friction coefficient [140]. Additionally, the oxidation–reduction process may change the surface morphology and rigidity, further regulating the friction behavior.

In 2019, Lang et al. proposed a novel method for controlling the friction properties of graphene using a C-AFM technique [141]. A negative bias was applied to the AFM probe to induce local electrochemical reactions on the graphene surface. This process produced oxygen functional groups that regulated the friction properties of graphene and enabled its controllable functionalization at the nanoscale. Studies have shown that the degree of functionalization could be precisely controlled by the probe voltage and contact time, and the friction coefficient of the functionalized area significantly increases (Figs. 10(a) and 10(b)). Moreover, after functionalization, the friction coefficient of graphene increases further when a bias is applied, which is attributed to the enhancement of capillary force and electrostatic force induced by the electric field (Fig. 10(c)).

In another study by the same team in 2021, the dynamic nanoscale friction behavior of graphene oxide (GO) under a positive bias condition was investigated using the C-AFM probe (Fig. 11(a)) [80]. It was found that the friction force of GO rapidly decreased in the initial scanning cycle and then gradually stabilized, which was attributed to the electrochemical reduction process of oxygen functional groups induced by the applied electric field. The bias size, relative humidity (RH), scanning speed, and normal load all affect the reduction degree and friction properties of GO (Figs. 11(b)–11(e)). A high humidity environment (72%RH) and a low scanning speed (1.5 μm/s) are more conducive to the reduction of GO, thereby significantly reducing the friction force. X-ray photoelectron spectroscopy (XPS) analysis confirmed that the hydrophilicity of the GO surface decreased after reduction, and the capillary force reduced.

The process of surface oxidation–reduction of 2D materials induced by electric fields is also influenced by the surface state of the 2D materials and external environmental factors. Zhang et al. (2020) studied the nanotribological properties of atomic-level steps on the surface of graphene under the action of an electric field (Fig. 12(a)) [142]. Through experiments, the authors found that the lateral friction force of uncovered step edges significantly increased with the increase in voltage, while the friction force of covered step edges only slightly increased with the increase in voltage. This was mainly attributed to the fact that the uncovered step edges were more prone to oxidation due to the adsorption of water molecules by the dangling bonds (Fig. 12(b)). The electric field enhanced the oxidation reaction at the step edges, especially at the uncovered step edges, where the oxidation degree was significantly higher than that at the covered step edges. The above study reveals the oxidation mechanism at the edge of the steps under the influence of an electric field. The adsorption of water molecules and chemical reactions are the key factors regulating the interface behavior. This naturally leads to an intriguing question: Could air humidity affect the friction and wear process of two-dimensional materials under the influence of an electric field? In a recent study, Tang et al. (2025) investigated the influence of humidity on the wear behavior of graphene under current conditions (Fig. 12(c)) [143]. Experiments showed that a high humidity environment (such as 90% relative humidity) could significantly slow down the wear of graphene, mainly through two mechanisms: One is to reduce the Joule heating effect, and the other is to reduce the oxidation of the carbon dangling bonds on the graphene surface by dissolving water molecules. The current accelerated the oxidation of graphene and the substrate (copper), while water molecules in the high humidity environment could effectively inhibit this process. Infrared thermal imaging and XPS analysis confirmed the regulatory effect of humidity on the temperature and chemical bond state of the friction interface.

The electrofield-induced redox reactions open up a novel avenue for the dynamic regulation of friction properties by altering the surface chemistry, morphology, and interfacial forces of 2D materials [144, 145]. Current research has preliminarily clarified the synergistic mechanism of electrofield parameters, surface structure, and environmental factors, but further exploration of the response differences of different 2D materials (such as MoS_2 and h-BN) and friction behaviors under extreme conditions (such as extremely high humidity, multi-physical field coupling) is still needed. In the future, by combining *in situ* characterization techniques with multi-scale simulations, it is expected to achieve precise prediction and optimization of friction properties, and promote the application of 2D materials in nanomechanics, intelligent lubrication, and other fields [146–148].

2.5 Mechanical resonance

The previous chapter discussed how the direct current (DC) electric field significantly influences the static or quasi-static interface friction behavior of 2D materials through mechanisms such as regulating charge carriers, inducing strain, enhancing electron–phonon coupling, or triggering redox reactions. However, the essence of friction is a dynamic process involving the relative motion of the contact interface and the instantaneous changes in energy dissipation [149–151]. To achieve more precise and real-time control of friction behavior and explore novel mechanisms beyond the effects of static electric fields, researchers have turned their attention to alternating current (AC) electric fields and the induced mechanical resonance phenomena [152].

Mechanical resonance refers to the physical phenomenon where

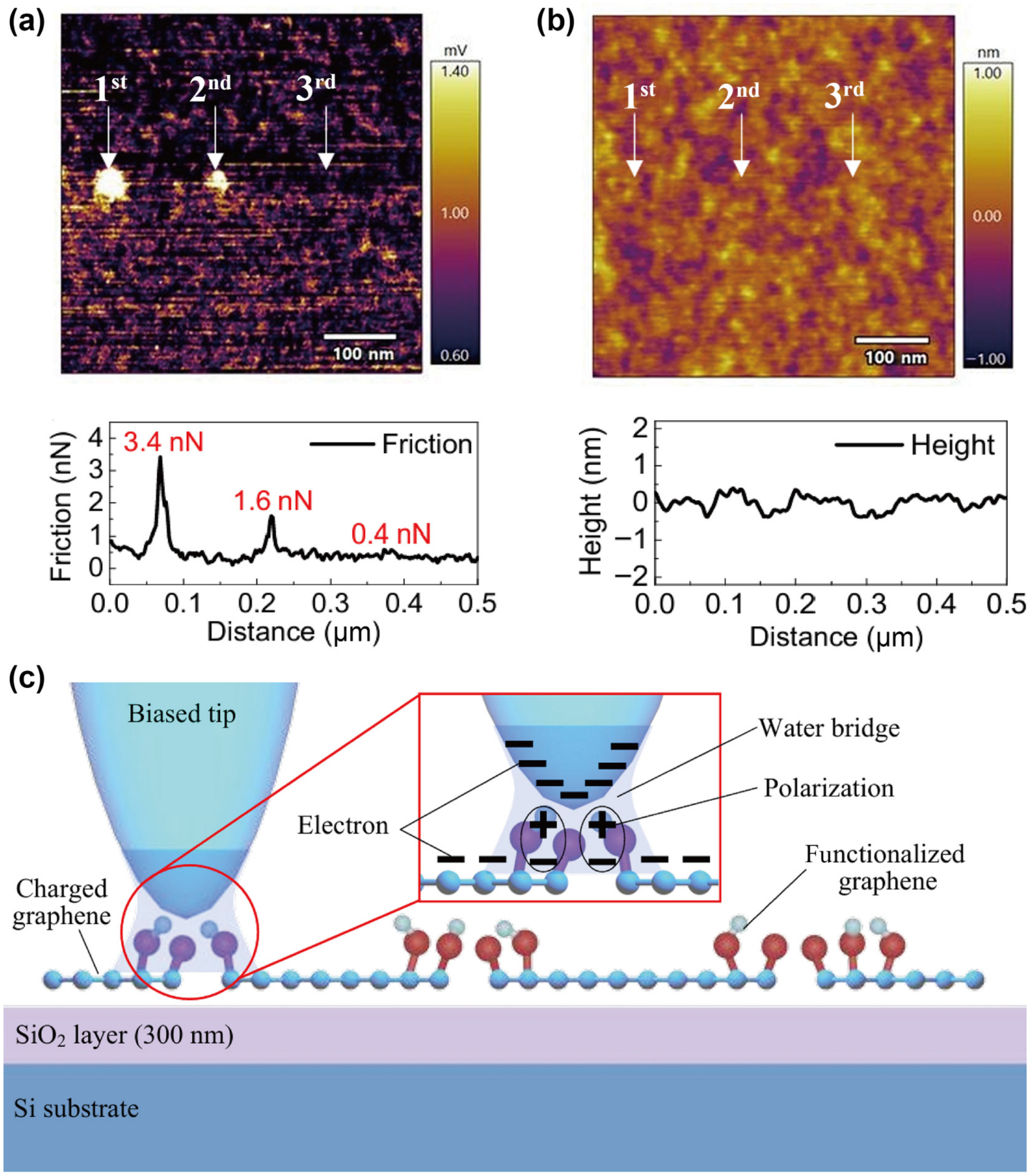

Figure 10 (a) Schematic diagram of AFM setup for functionalization of graphene deposited on SiO_2/Si substrate. (b) Frictional force (applied load of 1 nN) after functionalization. (c) Schematic of dynamic nanofriction using a positively biased conductive AFM tip. Reproduced with permission from Ref. [141], © The Royal Society of Chemistry 2019.

the amplitude of a system significantly increases when the external excitation frequency matches the system's natural frequency. In the field of nanotribology, stimulating the mechanical resonance of the probe-sample contact system or its supporting structure with AC electric fields provides a novel, dynamic, active control strategy for friction control. The core physical idea is that by applying a specific frequency (especially near the normal or lateral resonance frequency) of AC electric field, the contact interface or its adjacent area could be controllably excited with nanoscale vibrations. Compared to DC electric field regulation (mainly changing the static or quasi-static physical and chemical states of the interface), the mechanical vibration induced by AC electric field provides a dynamic control method. This method is non-destructive, highly responsive, and reversible. Under the influence of AC field, the materials are driven into a state of mechanical resonance, thereby potentially achieving ultra-low friction and even facilitating a state of structural superlubricity. It does not rely on the carrier transport or chemical reactions, and thus offers a novel way to control friction in material systems that have poor conductivity or are sensitive to electrochemistry.

Socoliuc et al. (2006) were the first to achieve active on–off control of atomic-scale friction. They accomplished this by stimulating the vertical mechanical resonance of the nano-contact system, and their work revealed the quantitative relationship between vibration amplitude and energy dissipation [153]. The authors used a friction force microscopy (FFM) in an ultra-high vacuum environment and conducted experiments on the surfaces of NaCl and KBr crystals. They found that by applying an alternating current voltage matching the normal resonance frequency of the system, within a specific excitation amplitude and load range, friction could be reduced to below 10 piconewtons without significant wear (Fig. 13(a)), and mechanical resonance

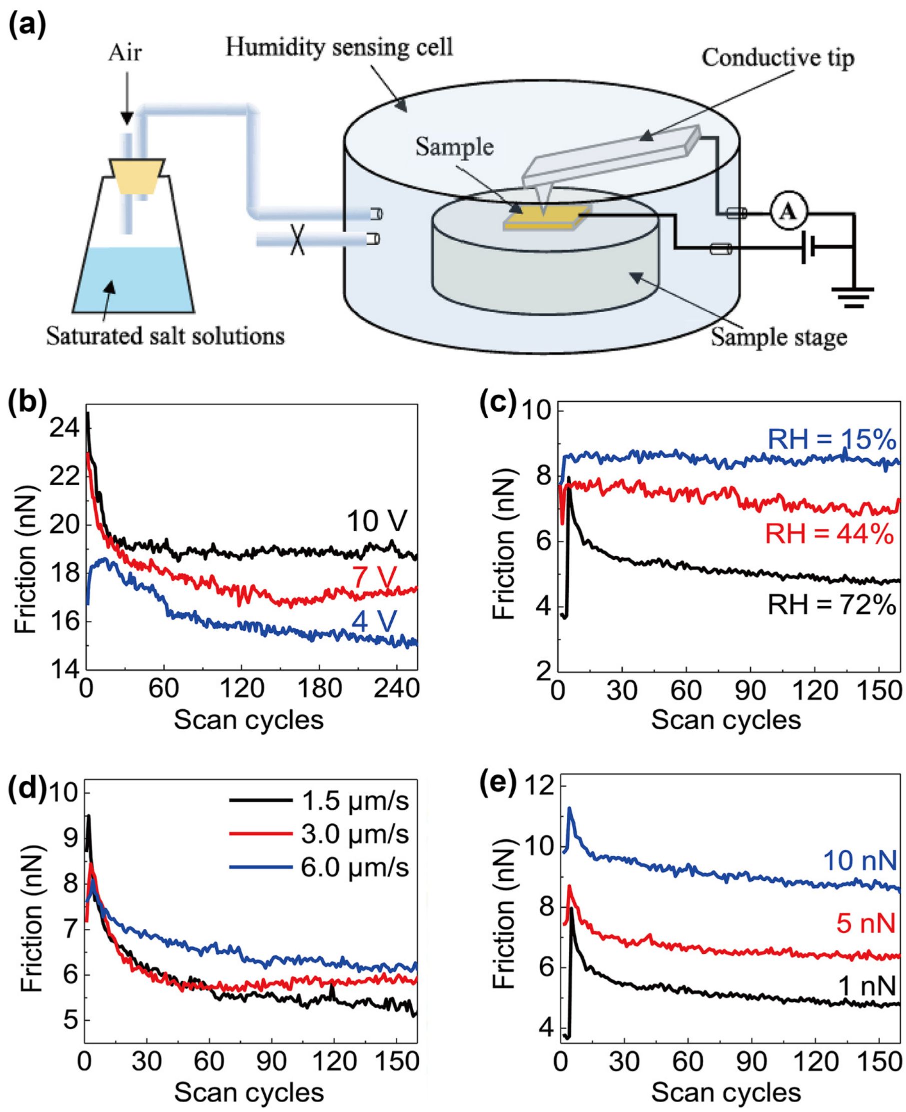

Figure 11 (a) Dynamic nanofriction force on GO under different voltages. (b) Schematic of the voltage-induced electrochemical reduction process. (c) Dynamic nanofriction force on GO under different RHs. (d) Dynamic nanofriction force on GO under different normal loads. (e) Dynamic nanofriction force on GO at different velocities. Reproduced with permission from Ref. [80], © American Chemical Society 2021.

could induce changes in the energy fluctuations of the contact interface, thereby suppressing the viscous sliding motion (Fig. 13(b)). Cao and Li (2022) used the inverse piezoelectric effect of piezoelectric films and only required an AC voltage below 10 V to generate nanoscale vibrations through contact resonance, reducing friction by more than 70% (Figs. 13(c) and 13(d)) [78]. Piezoelectric films generate nanoscale vibrations when subjected to AC electric fields. These vibrations become amplified through contact resonance, disturbing the fluctuation of sliding potential energy. As a result, viscous sliding motion is significantly suppressed, offering a novel concept for integrated friction control in micro-nano devices. Liu et al. (2025) further proposed a novel method for precisely controlling the friction of single-layer graphene interfaces by coupling DC and AC electric fields (Fig. 13(e)) [154]. The study found that by superimposing a low-amplitude AC electric field on top of the DC bias, the friction force could be continuously reduced by 75%, without damaging the integrity of the graphene interface. This effect is attributed to the unique energy dispersion mechanism induced by the electric field coupling, that is, the vertical resonance converts the horizontal sliding dissipation energy into vertical vibration energy. Subsequent simulations show that the horizontal dissipation energy ($\Delta P_x \approx -0.886$ μW) and the vertical absorption energy ($\Delta P_z \approx 0.889$ μW) are nearly equivalent in conversion, verifying the physical essence of energy directional dispersion (Fig. 13(f)). Three separate studies investigated the physical mechanism and technical pathway for controlling friction via AC-induced mechanical resonance. Each study approached the topic from a different angle: mechanical resonance, electric field coupling, and piezoelectric drive. Together, they establish a foundation for engineering super-lubricating interfaces based on 2D materials.

3 Prospects

Although significant progress has been made in the study of 2D material micro-scale current-carrying friction, there are still key challenges in the exploration of its fundamental theory and material systems [155–157]. In the future, it is necessary to systematically expand the material gene pool and go beyond traditional systems

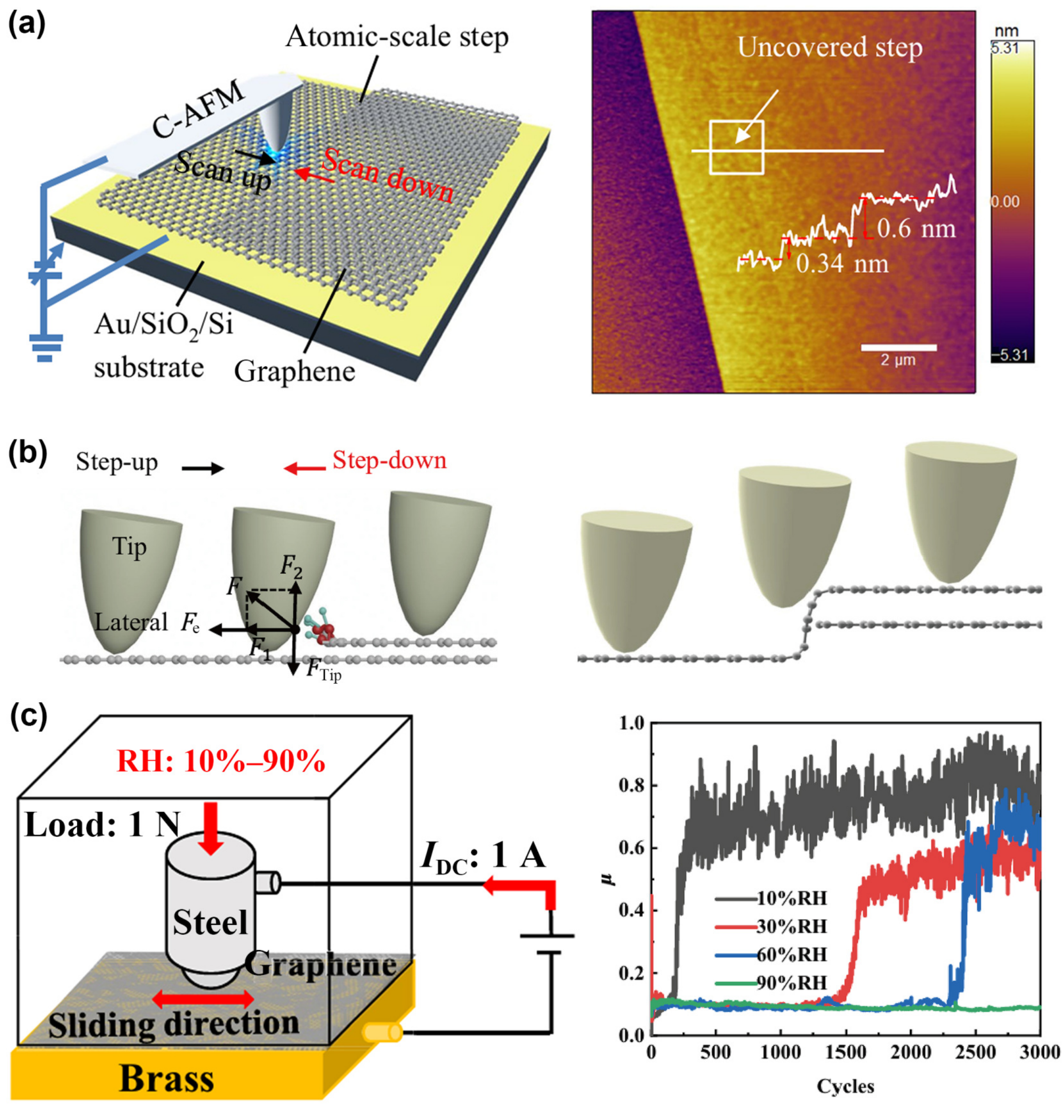

Figure 12 (a) Schematic of electric-carrying nanofriction experiments and topographic image of graphene with atomic step. (b) Force diagram of the AFM tip at uncovered step and covered step. Reproduced with permission from Ref. [142], © Springer Science+Business Media, LLC, part of Springer Nature 2020. (c) The schematic diagram with different humidity for the graphene film/steel ball friction interface, and friction coefficient under different humidity. Reproduced with permission from Ref. [143], © Tang, Q. et al. 2024.

such as graphene and MoS_2, to explore novel 2D materials with topological insulating states (Bi_2Se_3), magnetism (CrI_3), or superconducting properties ($NbSe_2$) under carrier conditions [78, 158, 159]. The unique electronic structure of such materials may give rise to novel friction control mechanisms, such as the quantum tunneling effect of topological surface states carriers on the interface barrier or the sudden change in viscous-slip behavior caused by superconducting phase transitions [160, 161].

In recent years, various new 2D materials have demonstrated great potential in ultra-low friction and intelligent control. For instance, He et al. fabricated large-area high-quality monolayer MoS_2 using the CVD method (Fig. 14(a)) [162]. The strong interfacial interaction between the material and the substrate significantly suppressed the wrinkling effect, achieving an extremely low friction coefficient of 0.00904, providing a new idea for designing ultrathin lubricating materials. Deng et al. reported the ternary 2D material $NiPS_3$, which exhibited an ultra-low friction coefficient of 0.0045 under high vacuum conditions (Fig. 14(b)) [163]. Its weak interlayer interaction and elimination of capillary force effect were the key factors for achieving this performance. In terms of gas regulation, Deng et al. further studied the friction behavior of single-layer $MoSe_2$ in different atmospheres, finding that its friction coefficient could be further reduced to 0.004 in pure N_2 environment (Fig. 14(c)), and the wear resistance life was increased by nearly four times, revealing the modulation effect of gas molecule adsorption on interface energy dissipation [164].

Existing mechanism studies mostly focus on ideal single-crystal materials, while the quantitative impact of defects (vacancies, grain boundaries, and folds) on current-carrying friction in actual devices has not yet been clarified [165–167]. It is necessary to combine *in situ* transmission electron microscopy–electrochemistry combined techniques, first-principles calculations, and cross-scale molecular dynamics simulations to reveal the synergistic effects of local electric field distortion [168–170], carrier scattering, and non-equilibrium phonon dissipation at defect sites, and to construct a universal theoretical model of "defect–electron–phonon" coupling.

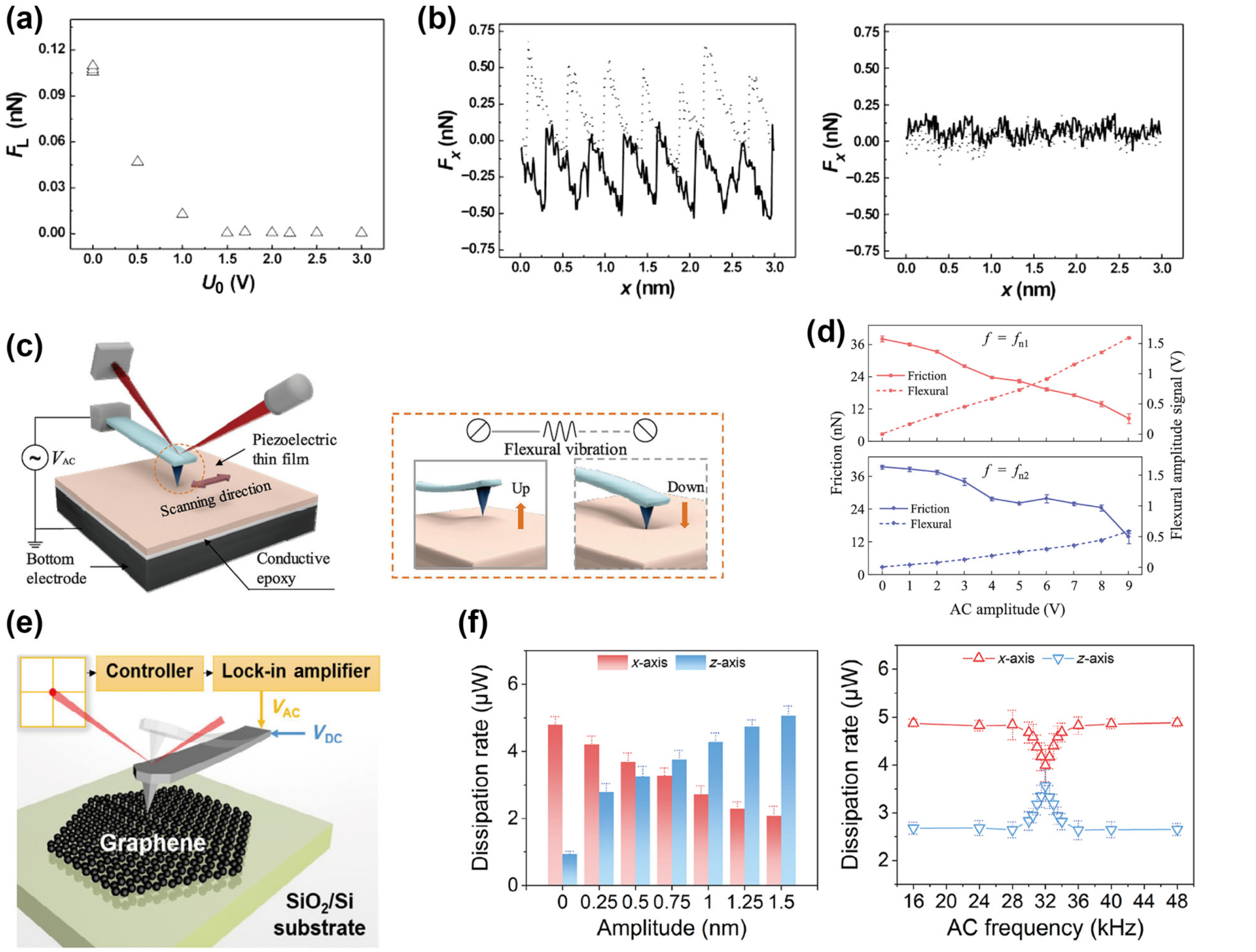

Figure 13 (a) Average frictional force as a function of the voltage amplitude U_0. (b) Before and after applying voltage, the lateral force on the surface of NaCl. Reproduced with permission from Ref. [153], © American Association for the Advancement of Science 2006. (c) A schematic diagram of the experimental setup for friction measurement under vibration actuation stemmin. (d) Variations of friction and flexural amplitude signal with actuation voltage amplitude. Reproduced with permission from Ref. [78], © Cao, J. W. et al. 2021. (e) Experimental illustration under the coupled DC/AC electric fields by contact mode electrostatic force microscopy (C-EFM). (f) The dependence of the potential energy dissipation rate P_x and P_z on amplitude and AC frequency. Reproduced with permission from Ref. [154], © Liu, Z. et al. 2025.

Moreover, the understanding of interface behavior under extreme conditions (such as ultra-low temperature and high current density) is still a blank area [77, 171, 172], and it is urgently necessary to develop low-temperature C-AFM and micro-Joule heat analysis platforms to clarify the reconfiguration laws of energy dissipation paths due to quantum confinement effects and thermal carrier injection in the long-term carrier operation [173–176].

For practical applications, the collaborative regulation of multiple physical fields and the integration of high-performance devices are the core directions to break through the technical bottlenecks [177–181]. The single-field regulation has response delay and energy consumption limitations. In the future, it is necessary to explore multi-field coupling strategies such as light-electro-magnetic-force coupling [182]: for example, using dynamic modulation of the Fermi level by photogenerated carriers combined with Lorentz force to suppress electron scattering; or achieving nanosecond-level switching of the friction coefficient through the vector superposition of piezoelectric strain field and electrostatic field [183–185]. Such coupling effects could significantly improve the regulation efficiency and provide a novel paradigm for intelligent lubrication systems. At the device level, three major issues need to be addressed: First, developing low-power friction switches that utilize mechanical resonance effects or phase-change materials (such as 1T′-$MoTe_2$) to design active control units with nanosecond response and picofarad-level energy consumption [186–188]. Second, overcoming the interface degradation problem during long-term carrier operation, by suppressing environmental oxidation through packaging technology and designing gradient heterojunctions (such as graphene/h-BN) to alleviate Joule heat accumulation [189, 190]. Third, promoting the deep integration of 2D material frictional properties and micro-nanoelectromechanical systems (MEMS/NEMS), such as using the strain–friction correlation in flexible electronics to achieve self-sensing drive [191–194]. In addition to 2D layered materials, other thin film materials can also be explored. Li et al. developed an air–liquid interface deposition technique, which achieved ultra-thin continuous conductive metal films with a thickness as low as 3.5 nm (Fig. 15(a)) [194]. These films exhibit excellent transparency, conductivity, and anti-wear properties. Additionally, they have created an electronic device that could monitor the bending of joints such as fingers, wrists, and arms (Figs. 15(b)–15(e)). This provides a new approach for integrating transparent

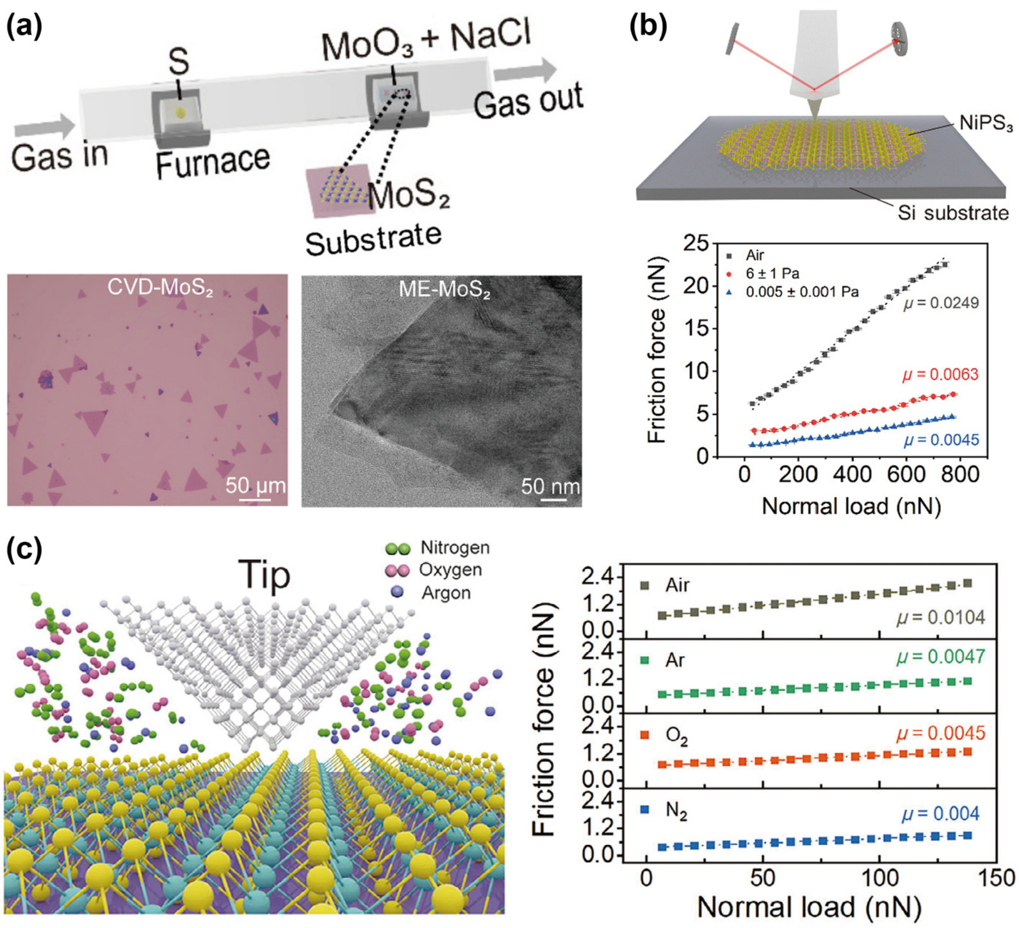

Figure 14 (a) Equipment schematic of a CVD system. Optical microscope image and TEM image of CVD-MoS_2. Reproduced with permission from Ref. [162], © He, X. J. et al. 2025. (b) The relationship between the friction force and the normal load of NPS nanosheets under different conditions. Reproduced with permission from Ref. [163], © Deng, H. Y. et al. 2024. (c) Frictional force as a function of normal load measured ML $MoSe_2$ under different atmospheres. Reproduced with permission from Ref. [164], © Wiley-VCH GmbH 2025.

electrodes and lubrication in flexible electronic devices. These breakthroughs require interdisciplinary collaboration, integration of microfabrication processes and *in situ* characterization techniques, and establishment of a full-chain design criteria from microscopic mechanisms to macroscopic devices [195].

In conclusion, the study of 2D material micro-scale current-carrying friction has significant scientific significance and application value. With the deepening of research, it is expected that more new phenomena, mechanisms, and applications would emerge, which would inject new vitality into the development of nanotribology and 2D materials [88, 196, 197].

4 Conclusions

This review has systematically examined the multiphysical mechanisms through which electric fields dynamically manipulate nanoscale friction in 2D materials. Moving beyond a simplistic view of friction as merely a mechanical phenomenon, we highlight that current-carrying friction constitutes a complex interplay of electronic, structural, chemical, and dynamic processes. The key insight unifying the discussed mechanisms is that an electric field acts as a versatile external stimulus that can precisely alter the interfacial energy dissipation pathways by modifying the charge distribution, lattice configuration, chemical state, and vibrational dynamics at the sliding interface.

The evolution of research in this field marks a significant transition from passive observation of frictional phenomena to active and tunable control. Table 1 summarizes the existing classic cases of electric field control of nanoscale friction in the academic community. Early studies established the foundational role of electrostatic effects and carrier concentration. Subsequent work revealed the importance of strain- and electron–phonon coupling-mediated dissipation. More recently, strategies involving electrochemical surface modification and, notably, AC field-induced mechanical resonance have opened avenues for dynamic, non-destructive, and ultra-low friction control, even in materials unsuitable for static field modulation.

Looking forward, the true potential lies in transitioning from understanding single mechanisms to designing synergistic, multi-field coupling strategies and in bridging the gap between atomistic-scale knowledge and reliable macroscale device performance. Future efforts must integrate cross-scale simulations, *in situ* diagnostics, and defect-engineered material synthesis to develop predictive models and robust interfaces. By consolidating the mechanistic insights outlined here, this review aims to provide a foundational framework for the rational design of 2D material-based devices where tailored frictional properties are crucial for enhancing reliability, efficiency, and functionality in next-generation nanoelectronics and MEMS/NEMS.

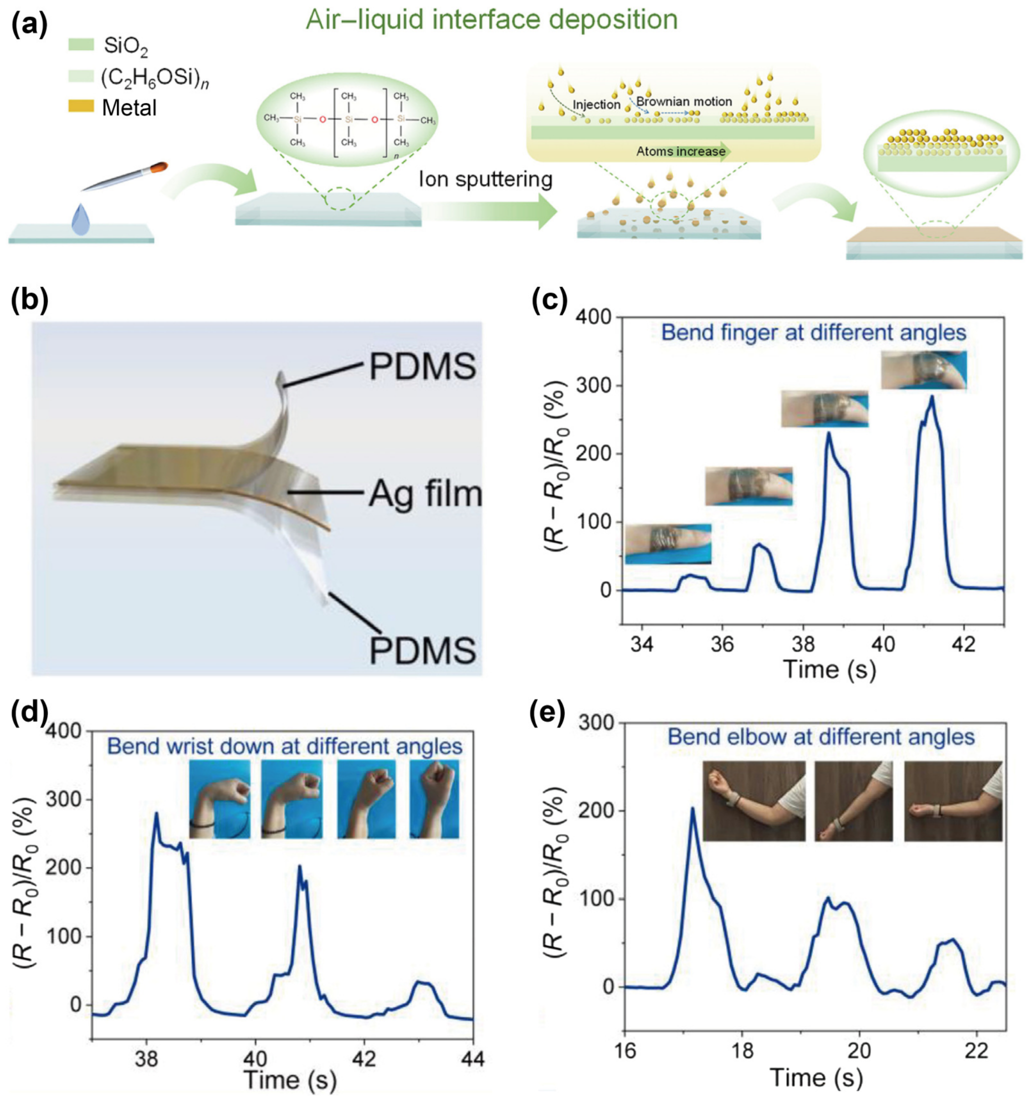

Figure 15 (a) Diagram of metal deposition at the air–liquid interface. (b) Schematic diagram of a flexible sensor element. (c) The test results of this device at the fingertip area. (d) The test results of this device on the back of the hand. (e) The test results of this device at the arm area. Reproduced with permission from Ref. [194], © Elsevier Ltd. 2025.

Table 1 The tribological behavior of typical two-dimensional materials under different electric field control mechanisms

Regulatory mechanism	Materials	Tribological behavior
Electrostatic effect	Graphene	Negative bias voltage can enhance friction.
	MoS_2	Electric fields can induce a state of ultra-low friction.
	h-BN	Negative bias enhances friction, and positive bias has a relatively weaker effect.
Electrostrictive strain	Graphene	The electric field causes lattice deformation, thereby reducing friction.
	MoS_2	The friction significantly decreases under the transverse electric field.
	ZIF-8	Both the longitudinal and transverse electric fields can significantly regulate friction.
Electron–phonon coupling	Graphene	The electroacoustic coupling of single-layer graphene is stronger, and friction is also higher.
	$MoSe_2$	The friction of n-type material significantly increases under a positive electric field.
	WSe_2	In p-type materials, the friction decreases under a positive electric field.
	$NbSe_2$	The friction increases with the increase of the bias voltage.
Oxidation–reduction induced by electric field	Graphene	Negative bias increases friction, and positive bias reduces friction.
	Graphene oxide	The friction force decreases under positive bias.
Mechanical resonance	NaCl/KBr	Inhibit the viscous sliding movement and reduce friction.
	Graphene	Vertical vibration energy conversion su PP resses horizontal dissipation and reduces friction.
	Piezoelectric film	Reduce friction through contact resonance.

Data availability

Not applicable.

Acknowledgements

Thanks for the financial support of the National Natural Science Foundation of China (Nos. 22309106, 52205230, 52275219, and 52205233), the Natural Science Foundation of Gansu Province (No. 23JRRA610), the Key Research and Development Program in Shandong Province (No. SYS202203), the Natural Science Foundation of Shandong Province (No. ZR2023QE067), and the Youth Innovation Technology Project of Higher School in Shandong Province (No. 2023KJ091).

Declaration of competing interest

The other contributing authors report no conflict of interests in this work.

Author contribution statement

Y. H. X.: Investigation, software, writing – original draft. S. L.: Supervision, visualization. L. Y. C.: Supervision, visualization. W. X. S.: Conceptualization, funding acquisition, methodology, writing – review & editing. D. A. W.: Project administration, resources, validation. All the authors have approved the final manuscript.

Use of AI statement

None.

References

[1] Novoselov, K. S.; Geim, A. K.; Morozov, S. V.; Jiang, D.; Zhang, Y.; Dubonos, S. V.; Grigorieva, I. V.; Firsov, A. A. Electric field effect in atomically thin carbon films. *Science* **2004**, *306*, 666–669.

[2] Soergel, E. Piezoresponse force microscopy (PFM). *J. Phys. D: Appl. Phys.* **2011**, *44*, 464003.

[3] Miao, H. C.; Sun, Y.; Zhou, X. L.; Li, Y. W.; Li, F. X. Piezoelectricity and ferroelectricity of cellular polypropylene electrets films characterized by piezoresponse force microscopy. *J. Appl. Phys.* **2014**, *116*, 066820.

[4] Yao, Q. Z.; Li, Q. Y. Line scan reconstruction: A viable approach for tracking atomic stick-slip events and true tip position in atomic force microscopy. *Tribol. Lett.* **2016**, *64*, 31.

[5] Ouyang, W. G.; Liu, X. Z.; Li, Q. Y.; Zhang, Y. Y.; Yang, J. R.; Zheng, Q. S. Optical methods for determining thicknesses of few-layer graphene flakes. *Nanotechnology* **2013**, *24*, 505701.

[6] Li, Q. Y.; Tullis, T. E.; Goldsby, D.; Carpick, R. W. Frictional ageing from interfacial bonding and the origins of rate and state friction. *Nature* **2011**, *480*, 233–236.

[7] Li, Q. Y.; Xia, K. L.; Zhang, J.; Zhang, Y. Y.; Li, Q. Y.; Takahashi, K.; Zhang, X. Measurement of specific heat and thermal conductivity of supported and suspended graphene by a comprehensive Raman optothermal method. *Nanoscale* **2017**, *9*, 10784–10793.

[8] Berman, D.; Erdemir, A.; Sumant, A. V. Approaches for achieving superlubricity in two-dimensional materials. *ACS Nano* **2018**, *12*, 2122–2137.

[9] Li, X. F.; Gao, T. T.; Wu, Y. Q. Development of two-dimensional materials for electronic applications. *Sci. China Inf. Sci.* **2016**, *59*, 061405.

[10] Solangi, N. H.; Karri, R. R.; Mubarak, N. M.; Mazari, S. A.; Azad, A. K. Emerging 2D MXenes as next-generation materials for energy storage applications. *J. Energy Storage* **2023**, *70*, 108004.

[11] Zhang, J.; Meguid, S. A. Piezoelectricity of 2D nanomaterials: Characterization, properties, and applications. *Semicond. Sci. Technol.* **2017**, *32*, 043006.

[12] Li, J. J.; Gao, T. Y.; Luo, J. B. Superlubricity of graphite induced by multiple transferred graphene nanoflakes. *Adv. Sci.* **2018**, *5*, 1700616.

[13] Marian, M.; Berman, D.; Rota, A.; Jackson, R. L.; Rosenkranz, A. Layered 2D nanomaterials to tailor friction and wear in machine elements—A review. *Adv. Mater. Interfaces* **2022**, *9*, 2101622.

[14] Hinchet, R.; Khan, U.; Falconi, C.; Kim, S. W. Piezoelectric properties in two-dimensional materials: Simulations and experiments. *Mater. Today* **2018**, *21*, 611–630.

[15] Li, J. J.; Li, J. F.; Luo, J. B. Superlubricity of graphite sliding against graphene nanoflake under ultrahigh contact pressure. *Adv. Sci.* **2018**, *5*, 1800810.

[16] Wang, Y.; Cheng, Y.; Wang, Y. L.; Zhang, S.; Zhang, X. W.; Yin, S. Q.; Wang, M.; Xia, Y.; Li, Q. Y.; Zhao, P. et al. Oxide-assisted growth of scalable single-crystalline graphene with seamlessly stitched millimeter-sized domains on commercial copper foils. *RSC Adv.* **2018**, *8*, 8800–8804.

[17] Wang, Z. G.; Li, Q.; Xu, H. X.; Dahl-Petersen, C.; Yang, Q.; Cheng, D. J.; Cao, D. P.; Besenbacher, F.; Lauritsen, J. V.; Helveg, S. et al. Controllable etching of MoS_2 basal planes for enhanced hydrogen evolution through the formation of active edge sites. *Nano Energy* **2018**, *49*, 634–643.

[18] Geim, A. K.; Novoselov, K. S. The rise of graphene. *Nat. Mater.* **2007**, *6*, 183–191.

[19] Zeng, Y. M.; He, F.; Wang, Q.; Yan, X. H.; Xie, G. X. Friction and wear behaviors of molybdenum disulfide nanosheets under normal electric field. *Appl. Surf. Sci.* **2018**, *455*, 527–532.

[20] Han, S. A.; Lee, J.; Lin, J. J.; Kim, S. W.; Kim, J. H. Piezo/triboelectric nanogenerators based on 2-dimensional layered structure materials. *Nano Energy* **2019**, *57*, 680–691.

[21] Shao, Y.; Song, S. R.; Wu, X.; Qi, J.; Lu, H. L.; Liu, C.; Zhu, S. Y.; Liu, Z. L.; Wang, J. O.; Shi, D. X. et al. Epitaxial fabrication of two-dimensional $NiSe_2$ on Ni (111) substrate. *Appl. Phys. Lett.* **2017**, *111*, 113107.

[22] Huang, M.; Biswal, M.; Park, H. J.; Jin, S.; Qu, D. S.; Hong, S.; Zhu, Z. L.; Qiu, L.; Luo, D.; Liu, X. C. et al. Highly oriented monolayer graphene grown on a Cu/Ni (111) alloy foil. *ACS Nano* **2018**, *12*, 6117–6127.

[23] Li, Z. F.; Xi, X. K.; Ding, B.; Li, H.; Liu, E. K.; Yao, Y.; Wang, W. H. Thermodynamics and kinetics synergy for controlled synthesis of 2D van der Waals single-crystal $NbSe_2$ via modified chemical vapor transport. *Cryst. Growth Des.* **2020**, *20*, 706–712.

[24] Hachiya, R.; Urakami, N.; Hashimoto, Y. Direct growth of $NbSe_2$ and $TiSe_2$ thin flakes via deposited film selenization. *Jpn. J. Appl. Phys.* **2020**, *59*, SCCB25.

[25] Mo, Y. F.; Turner, K. T.; Szlufarska, I. Friction laws at the nanoscale. *Nature* **2009**, *457*, 1116–1119.

[26] Meng, Y. G.; Xu, J.; Jin, Z. M.; Prakash, B.; Hu, Y. Z. A review of recent advances in tribology. *Friction* **2020**, *8*, 221–300.

[27] Bennewitz, R. Friction force microscopy. *Mater. Today* **2005**, *8*, 42–48.

[28] Liu, L. C.; Zhou, M.; Jin, L.; Li, L. C.; Mo, Y. T.; Su, G. S.; Li, X.; Zhu, H. W.; Tian, Y. Recent advances in friction and lubrication of graphene and other 2D materials: Mechanisms and applications. *Friction* **2019**, *7*, 199–216.

[29] Lee, C.; Wei, X. D.; Li, Q. Y.; Carpick, R.; Kysar, J. W.; Hone, J. Elastic and frictional properties of graphene. *Phys. Status Solidi (B)* **2009**, *246*, 2562–2567.

[30] Li, Q. Y.; Lee, C.; Carpick, R. W.; Hone, J. Substrate effect on

thickness-dependent friction on graphene. *Phys. Status Solidi (B)* **2010**, *247*, 2909–2914.

[31] Dong, Y.; Li, Q.; Wu, J.; Martini, A. Friction, slip and structural inhomogeneity of the buried interface. *Modell. Simul. Mater. Sci. Eng.* **2011**, *19*, 065003.

[32] Zhang, D. L.; Li, Z. B.; Klausen, L. H.; Li, Q.; Dong, M. D. Friction behaviors of two-dimensional materials at the nanoscale. *Mater. Today Phys.* **2022**, *27*, 100771.

[33] Cao, X. A.; Gan, X. H.; Lang, H. J.; Peng, Y. T. Impact of the surface and microstructure on the lubricative properties of MoS_2 aging under different environments. *Langmuir* **2021**, *37*, 2928–2941.

[34] Zhang, S.; Ma, T. B.; Erdemir, A.; Li, Q. Y. Tribology of two-dimensional materials: From mechanisms to modulating strategies. *Mater. Today* **2019**, *26*, 67–86.

[35] Li, Q. Y.; Dong, Y. L.; Martini, A.; Carpick, R. W. Atomic friction modulation on the reconstructed Au (111) surface. *Tribol. Lett.* **2011**, *43*, 369–378.

[36] Li, Q. Y.; Dong, Y. L.; Perez, D.; Martini, A.; Carpick, R. W. Speed dependence of atomic stick-slip friction in optimally matched experiments and molecular dynamics simulations. *Phys. Rev. Lett.* **2011**, *106*, 126101.

[37] Liu, X. Z.; Li, Q. Y.; Egberts, P.; Carpick, R. W. Nanoscale adhesive properties of graphene: The effect of sliding history. *Adv. Mater. Interfaces* **2014**, *1*, 1300053.

[38] Sun, X. Y.; Qi, Y. Z.; Ouyang, W. G.; Feng, X. Q.; Li, Q. Y. Energy corrugation in atomic-scale friction on graphite revisited by molecular dynamics simulations. *Acta Mech. Sin.* **2016**, *32*, 604–610.

[39] Li, S. Z.; Li, Q. Y.; Carpick, R. W.; Gumbsch, P.; Liu, X. Z.; Ding, X. D.; Sun, J.; Li, J. The evolving quality of frictional contact with graphene. *Nature* **2016**, *539*, 541–545.

[40] Ye, S.; Li, B.; Li, Q. Y.; Zhao, H. P.; Feng, X. Q. Deep neural network method for predicting the mechanical properties of composites. *Appl. Phys. Lett.* **2019**, *115*, 161901.

[41] Wang, D.; Tan, C.; Wang, S. Y.; Yang, Z. H.; Yang, L.; Wang, Z. G. Sm and Gd contacts in 2D semiconductors for high-performance electronics and spintronics. *ACS Appl. Mater. Interfaces* **2024**, *16*, 14064–14071.

[42] Sun, K.; Diao, D. F. Current density effect on current-carrying friction of amorphous carbon film. *Carbon* **2020**, *157*, 113–119.

[43] Lang, H. J.; Peng, Y. T.; Cao, X. A.; Zou, K. Atomic-scale friction characteristics of graphene under conductive AFM with applied voltages. *ACS Appl. Mater. Interfaces* **2020**, *12*, 25503–25511.

[44] Zheng, X. H.; Gao, L.; Yao, Q. Z.; Li, Q. Y.; Zhang, M.; Xie, X. M.; Qiao, S.; Wang, G.; Ma, T. B.; Di, Z. F. et al. Robust ultra-low-friction state of graphene via moiré superlattice confinement. *Nat. Commun.* **2016**, *7*, 13204.

[45] Zhao, J.; Peng, Y. T.; Zhou, Q. G.; Zou, K. The current-carrying tribological properties of Cu/graphene composites. *J. Tribol.* **2021**, *143*, 102101.

[46] Huang, Y. H.; Yao, Q. Z.; Qi, Y. Z.; Cheng, Y.; Wang, H. T.; Li, Q. Y.; Meng, Y. G. Wear evolution of monolayer graphene at the macroscale. *Carbon* **2017**, *115*, 600–607.

[47] Lang, J. L.; Ding, B.; Zhang, S.; Su, H. X.; Ge, B. H.; Qi, L. H.; Gao, H. J.; Li, X. Y.; Li, Q. Y.; Wu, H. Scalable synthesis of 2D Si nanosheets. *Adv. Mater.* **2017**, *29*, 1701777.

[48] Pace, G.; del Rio Castillo, A. E.; Lamperti, A.; Lauciello, S.; Bonaccorso, F. 2D materials-based electrochemical triboelectric nanogenerators. *Adv. Mater.* **2023**, *35*, 2211037

[49] Choi, Y. S.; Kim, S. W.; Kar-Narayan, S. Materials-related strategies for highly efficient triboelectric energy generators. *Adv. Energy Mater.* **2021**, *11*, 2003802.

[50] Huo, Z. W.; Wei, Y. C.; Wang, Y. F.; Wang, Z. L.; Sun, Q. J. Integrated self-powered sensors based on 2D material devices. *Adv. Funct. Mater.* **2022**, *32*, 2206900.

[51] Huo, Z. W.; Yu, J. R.; Li, Y. H.; Wang, Z. L.; Sun, Q. J. 2D tribotronic transistors. *J. Phys. : Energy* **2023**, *5*, 012002.

[52] Zhong, H. K.; Wu, Z. Q.; Li, X. Q.; Xu, W. L.; Xu, S.; Zhang, S. J.; Xu, Z. J.; Chen, H. S.; Lin, S. S. Graphene based two dimensional hybrid nanogenerator for concurrently harvesting energy from sunlight and water flow. *Carbon* **2016**, *105*, 199–204.

[53] Liu, J.; Zhang, S.; Li, Q. Y.; Feng, X. Q.; Di, Z. F.; Ye, C.; Dong, Y. L. Lateral force modulation by moiré superlattice structure: Surfing on periodically undulated graphene sheets. *Carbon* **2017**, *125*, 76–83.

[54] Fan, X. G.; He, C.; Ding, J.; Gao, Q.; Ma, H. L.; Lemme, M. C.; Zhang, W. D. Graphene MEMS and NEMS. *Microsyst. Nanoeng.* **2024**, *10*, 154.

[55] Smith, A. D.; Niklaus, F.; Paussa, A.; Vaziri, S.; Fischer, A. C.; Sterner, M.; Forsberg, F.; Delin, A.; Esseni, D.; Palestri, P. et al. Electromechanical piezoresistive sensing in suspended graphene membranes. *Nano Lett.* **2013**, *13*, 3237–3242.

[56] Smith, A. D.; Niklaus, F.; Paussa, A.; Schröder, S.; Fischer, A. C.; Sterner, M.; Wagner, S.; Vaziri, S.; Forsberg, F.; Esseni, D. et al. Piezoresistive properties of suspended graphene membranes under uniaxial and biaxial strain in nanoelectromechanical pressure sensors. *ACS Nano* **2016**, *10*, 9879–9886.

[57] Goodson, H. E. Electric charges by friction. *Nature* **1924**, *114*, 159–159.

[58] Medley, J. A. Frictional electrification and gaseous discharge. *Nature* **1950**, *166*, 524–525.

[59] Park, J. Y.; Ogletree, D. F.; Thiel, P. A.; Salmeron, M. Electronic control of friction in silicon pn junctions. *Science* **2006**, *313*, 186–186.

[60] Butler, S. Z.; Hollen, S. M.; Cao, L. Y.; Cui, Y.; Gupta, J. A.; Gutiérrez, H. R.; Heinz, T. F.; Hong, S. S.; Huang, J. X.; Ismach, A. F. et al. Progress, challenges, and opportunities in two-dimensional materials beyond graphene. *ACS Nano* **2013**, *7*, 2898–2926.

[61] Zuo, Y. G.; Liu, C.; Ding, L. P.; Qiao, R. X.; Tian, J. P.; Liu, C.; Wang, Q. H.; Xue, G. D.; You, Y. L.; Guo, Q. L. et al. Robust growth of two-dimensional metal dichalcogenides and their alloys by active chalcogen monomer supply. *Nat. Commun.* **2022**, *13*, 1007.

[62] Wang, Y. N.; Zhao, C.; Gao, X.; Zheng, L. M.; Qian, J.; Gao, X. Y.; Li, J. D.; Tang, J. C.; Tan, C. W.; Wang, J. H. et al. Ultraflat single-crystal hexagonal boron nitride for wafer-scale integration of a 2D-compatible high-κ metal gate. *Nat. Mater.* **2024**, *23*, 1495–1501.

[63] Yang, Y.; Wang, G.; Zhou, X. C.; Su, X. K.; Gu, L. A promising conductive lubricant for space sliding electrical contact: $NbSe_2$-Ti film. *Lubricants* **2024**, *12*, 44.

[64] Zheng, Q. S.; Jiang, B.; Liu, S. P.; Weng, Y. X.; Lu, L.; Xue, Q. K.; Zhu, J.; Jiang, Q.; Wang, S.; Peng, L. M. Self-retracting motion of graphite microflakes. *Phys. Rev. Lett.* **2008**, *100*, 067205.

[65] Liu, Z.; Zheng, Q. S.; Liu, J. Z. Stripe/kink microstructures formed in mechanical peeling of highly orientated pyrolytic graphite. *Appl. Phys. Lett.* **2010**, *96*, 201909.

[66] Shi, R. Y.; Gao, L.; Lu, H. L.; Li, Q. Y.; Ma, T. B.; Guo, H.; Du, S. X.; Feng, X. Q.; Zhang, S.; Liu, Y. M. et al. Moiré superlattice-level stick-slip instability originated from geometrically corrugated graphene on a strongly interacting substrate. *2D Mater.* **2017**, *4*, 025079.

[67] Huang, Y. H.; Yao, Q. Z.; Lu, Z. X.; Jiao, L. Y.; Zhang, S.; Li, Q. Y.; Meng, Y. G. Antiwear performance of monolayer MoS_2 modulated by residual straining. *ACS Appl. Nano Mater.* **2018**, *1*, 7092–7097.

[68] Sun, J. H.; Zhang, Y. N.; Lu, Z. B.; Li, Q. Y.; Xue, Q. J.; Du, S. Y.; Pu, J. B.; Wang, L. P. Superlubricity enabled by pressure-induced friction collapse. *J. Phys. Chem. Lett.* **2018**, *9*, 2554–2559.

[69] Liu, Z.; Bøggild, P.; Yang, J. R.; Cheng, Y.; Grey, F.; Liu, Y. L.; Wang, L.; Zheng, Q. S. A graphite nanoeraser. *Nanotechnology* **2011**, *22*, 265706.

[70] Liu, Z.; Liu, J. Z.; Cheng, Y.; Li, Z. H.; Wang, L.; Zheng, Q. S. Interlayer binding energy of graphite: A mesoscopic determination from deformation. *Phys. Rev. B* **2012**, *85*, 205418.

[71] Liu, Z.; Yang, J. R.; Grey, F.; Liu, J. Z.; Liu, Y. L.; Wang, Y. B.; Yang, Y. L.; Cheng, Y.; Zheng, Q. S. Observation of microscale superlubricity in graphite. *Phys. Rev. Lett.* **2012**, *108*, 205503.

[72] Luo, J.; Ouyang, W. G.; Li, X. P.; Jin, Z.; Yang, L. J.; Chen, C. Q.; Zhang, J.; Li, Y.; Warner, J. H.; Peng, L. M. et al. Pointwise plucking of suspended carbon nanotubes. *Nano Lett.* **2012**, *12*, 3663–3667.

[73] Wang, L. F.; Ma, T. B.; Hu, Y. Z.; Zheng, Q. S.; Wang, H.; Luo, J. B. Superlubricity of two-dimensional fluorographene/MoS_2 heterostructure: A first-principles study. *Nanotechnology* **2014**, *25*, 385701.

[74] Zheng, Q. S.; Liu, Z. Experimental advances in superlubricity. *Friction* **2014**, *2*, 182–192.

[75] Peng, Y. T.; Zeng, X. Z.; Yu, K.; Lang, H. J. Deformation induced atomic-scale frictional characteristics of atomically thin two-dimensional materials. *Carbon* **2020**, *163*, 186–196.

[76] Yu, K. M.; Zou, K.; Lang, H. J.; Peng, Y. T. Nanofriction characteristics of h-BN with electric field induced electrostatic interaction. *Friction* **2021**, *9*, 1492–1503.

[77] Zhang, S.; Hou, Y.; Li, S. Z.; Liu, L. Q.; Zhang, Z.; Feng, X. Q.; Li, Q. Y. Tuning friction to a superlubric state via in-plane straining. *Proc. Natl. Acad. Sci. USA* **2019**, *116*, 24452–24456.

[78] Cao, J. W.; Li, Q. Y. Vibration-induced nanoscale friction modulation on piezoelectric materials. *Friction* **2022**, *10*, 1650–1659.

[79] Greenwood, G.; Kim, J. M.; Nahid, S. M.; Lee, Y.; Hajarian, A.; Nam, S.; Espinosa-Marzal, R. M. Dynamically tuning friction at the graphene interface using the field effect. *Nat. Commun.* **2023**, *14*, 5801.

[80] Lang, H. J.; Yu, M. C.; Peng, Y. T.; Zhao, X. H.; Zou, K. Dynamic nanofriction of graphene oxide induced by a positively biased conductive AFM tip. *J. Phys. Chem. C* **2021**, *125*, 18334–18340.

[81] Liu, P. F.; Yu, T. T.; Du, C. H.; Deng, H. Y.; He, X. J.; Li, S.; Xu, D. H.; Wang, Y. Q.; Wang, D. A. Nanofriction modulation under electric field based on 2D SiP. *Tribol. Int.* **2026**, *213*, 111069.

[82] Zou, J. D.; Zhu, R. D.; Wang, J. Y.; Meng, H. T.; Wang, Z.; Chen, H. L.; Weng, Y. X. Coherent phonon-mediated many-body interaction in monolayer WSe_2. *J. Phys. Chem. Lett.* **2023**, *14*, 4657–4665.

[83] Wang, W.; Dai, S. Y.; Li, X. D.; Yang, J. R.; Srolovitz, D. J.; Zheng, Q. S. Measurement of the cleavage energy of graphite. *Nat. Commun.* **2015**, *6*, 7853.

[84] Deng, H.; Ma, M.; Song, Y. M.; He, Q. C.; Zheng, Q. S. Structural superlubricity in graphite flakes assembled under ambient conditions. *Nanoscale* **2018**, *10*, 14314–14320.

[85] Gongyang, Y. J.; Qu, C. Y.; Zhang, S. M.; Ma, M.; Zheng, Q. S. Eliminating delamination of graphite sliding on diamond-like carbon. *Carbon* **2018**, *132*, 444–450.

[86] Hod, O.; Meyer, E.; Zheng, Q. S.; Urbakh, M. Structural superlubricity and ultralow friction across the length scales. *Nature* **2018**, *563*, 485–492.

[87] Liu, B. T.; Wang, J.; Peng, X. N.; Qu, C. Y.; Ma, M.; Zheng, Q. S. Direct fabrication of graphite-mica heterojunction and *in situ* control of their relative orientation. *Mater. Des.* **2018**, *160*, 371–376.

[88] Liu, L.; Zhou, W.; Peng, Y. T.; Jiao, S. L.; Huang, Y. Z.; Lv, J. Enhanced lubrication and photocatalytic degradation of liquid paraffin by hollow MoS_2 microspheres. *ACS Omega* **2018**, *3*, 3120–3128.

[89] Mattinen, M.; Hatanpää, T.; Sarnet, T.; Mizohata, K.; Meinander, K.; King, P. J.; Khriachtchev, L.; Räisänen, J.; Ritala, M.; Leskelä, M. Atomic layer deposition of crystalline MoS_2 thin films: New molybdenum precursor for low-temperature film growth. *Adv. Mater. Interfaces* **2017**, *4*, 1700123.

[90] Hu, H.; Shi, B.; Breslin, C. M.; Gignac, L.; Peng, Y. T. A sub-micron spherical atomic force microscopic tip for surface measurements. *Langmuir* **2020**, *36*, 7861–7867.

[91] Lang, H. J.; Peng, Y. T.; Cao, X. A.; Yu, K. Dynamic electron transfer for reducing nanofriction of graphene at electrified interfaces. *Appl. Surf. Sci.* **2020**, *520*, 146327.

[92] Shi, B.; Gan, X. H.; Zhang, C.; Lang, H. J.; Zou, K.; Bu, T. Z.; Peng, Y. T. Investigating the effect of nanoscale triboelectrification on nanofriction in insulators. *Nano Energy* **2022**, *91*, 106620.

[93] Gong, P.; Li, Q. Y.; Liu, X. Z.; Carpick, R. W.; Egberts, P. Adhesion mechanics between nanoscale silicon oxide tips and few-layer graphene. *Tribol. Lett.* **2017**, *65*, 61.

[94] Wang, W.; Zhang, Y.; Li, Z. H.; Qian, L. M. Controllable friction on graphene via adjustable interfacial contact quality. *Adv. Sci.* **2023**, *10*, 2303013.

[95] Gongyang, Y. J.; Ouyang, W. G.; Qu, C. Y.; Urbakh, M.; Quan, B. G.; Ma, M.; Zheng, Q. S. Temperature and velocity dependent friction of a microscale graphite-DLC heterostructure. *Friction* **2020**, *8*, 462–470.

[96] Burgo, T. A. L.; Silva, C. A.; Balestrin, L. B. S.; Galembeck, F. Friction coefficient dependence on electrostatic tribocharging. *Sci. Rep.* **2013**, *3*, 2384.

[97] Jeong, J. H.; Jung, Y.; Park, J. U.; Lee, G. H. Gate-tunable electrostatic friction of grain boundary in chemical-vapor-deposited MoS_2. *Nano Lett.* **2023**, *23*, 3085–3089.

[98] Su, H. Y.; Zhang, H. L.; Sun, J. H.; Lang, H. J.; Zou, K.; Peng, Y. T. Reversible and controllable reduction in friction of atomically thin two-dimensional materials through high-stress pre-rubbing. *Nat. Commun.* **2024**, *15*, 9897.

[99] Huang, Y. Z.; Liu, L.; Yang, J. J.; Chen, Y. F. Nanotribological properties of ALD-made ultrathin MoS_2 influenced by film thickness and scanning velocity. *Langmuir* **2019**, *35*, 3651–3657.

[100] Liu, X. F.; Li, Y.; Guo, W. L. Friction modulation via photoexcitation in two-dimensional materials. *ACS Appl. Mater. Interfaces* **2020**, *12*, 2910–2915.

[101] Qu, C. Y.; Cao, W.; Liu, B. T.; Wang, A. L.; Xie, F. K.; Ma, M.; Shan, W. Z.; Urbakh, M.; Zheng, Q. S. Direct measurement of adhesions of liquids on graphite. *J. Phys. Chem. C* **2019**, *123*, 11671–11676.

[102] Shi, B.; Gan, X. H.; Lang, H. J.; Zou, K.; Wang, L. F.; Sun, J. H.; Lu, Y. Y.; Peng, Y. T. Ultra-low friction and patterning on atomically thin MoS_2 via electronic tight-binding. *Nanoscale* **2021**, *13*, 16860–16871.

[103] Chen, W. B.; Tang, C. W.; Li, T. Y.; Zou, X. L.; Zhang, J.; Jia, S.; Yuan, J. T.; George, A.; Voronine, D.; Ajayan, P. et al. Tunable friction of monolayer MoS_2 by control of interfacial chemistry. *Extrem. Mech. Lett.* **2020**, *41*, 100996.

[104] Park, J. Y.; Qi, Y. B.; Ogletree, D. F.; Thiel, P. A.; Salmeron, M. Influence of carrier density on the friction properties of siliconpnjunctions. *Phys. Rev. B* **2007**, *76*, 064108.

[105] Shi, B.; Gan, X. H.; Yu, K.; Lang, H. J.; Cao, X. A.; Zou, K.; Peng, Y. T. Electronic friction and tuning on atomically thin MoS_2. *npj 2D Mater. Appl.* **2022**, *6*, 39.

[106] Qiao, H. M.; Zhao, P.; Kwon, O.; Sohn, A.; Zhuo, F. P.; Lee, D. M.; Sun, C.; Seol, D.; Lee, D.; Kim, S. W. et al. Mixed triboelectric and flexoelectric charge transfer at the nanoscale. *Adv. Sci.* **2021**, *8*, 2101793.

[107] Li, B. Y.; Xu, M. Y.; Zhang, D. L.; Zhang, Y. G.; Li, Q.; Dong, M. D. Current-carrying friction of atomically thin molybdenum disulfide. *Appl. Surf. Sci.* **2025**, *685*, 162021.

[108] Wang, J. H.; Li, D.; Fan, Y.; Shi, M. H.; Yang, Y. X.; Wang, L.; Peng, Y. T.; Shen, M. W.; Shi, X. Y. Core–shell tecto dendrimers formed via host–guest supramolecular assembly as pH-responsive intelligent carriers for enhanced anticancer drug delivery. *Nanoscale* **2019**, *11*, 22343–22350.

[109] Wang, K. Q.; Qu, C. Y.; Wang, J.; Ouyang, W. G.; Ma, M.; Zheng, Q. S. Strain engineering modulates graphene interlayer friction by

Moiré pattern evolution. *ACS Appl. Mater. Interfaces* **2019**, *11*, 36169–36176.

[110] Wang, L.; Xu, X. Z.; Zhang, L. N.; Qiao, R. X.; Wu, M. H.; Wang, Z. C.; Zhang, S.; Liang, J.; Zhang, Z. H.; Zhang, Z. B. et al. Epitaxial growth of a 100-square-centimetre single-crystal hexagonal boron nitride monolayer on copper. *Nature* **2019**, *570*, 91–95.

[111] Si, C.; Sun, Z. M.; Liu, F. Strain engineering of graphene: A review. *Nanoscale* **2016**, *8*, 3207–3217.

[112] Zhao, X. H.; Xu, W.; Yi, W. M.; Peng, Y. T. A flexible and highly pressure-sensitive PDMS sponge based on silver nanoparticles decorated reduced graphene oxide composite. *Sens. Actuators A: Phys.* **2019**, *291*, 23–31.

[113] He, F.; Yang, X.; Bian, Z. L.; Xie, G. X.; Guo, D.; Luo, J. B. In-plane potential gradient induces low frictional energy dissipation during the stick-slip sliding on the surfaces of 2D mater. *Small* **2019**, *15*, 1904613.

[114] Li, Y. X.; Liu, L.; Song, A. S.; Wang, K. P.; Liu, Y. H. Electrotunable superlubricity of two-dimensional ZIF-8. *Carbon* **2025**, *232*, 119803.

[115] Yan, J.; Zhang, Y. B.; Kim, P.; Pinczuk, A. Electric field effect tuning of electron–phonon coupling in graphene. *Phys. Rev. Lett.* **2007**, *98*, 166802.

[116] Lai, J. M.; Xie, Y. R.; Zhang, J. Detection of electron–phonon coupling in two-dimensional materials by light scattering. *Nano Res.* **2021**, *14*, 1711–1733.

[117] Al Taleb, A.; Wan, W.; Benedek, G.; Ugeda, M. M.; Farías, D. Electron–phonon coupling and phonon dynamics in single-layer $NbSe_2$ on graphene: The role of Moiré phonons. *ACS Nano* **2025**, *19*, 8895–8903.

[118] Stajic, J. A timely look into electron–phonon coupling. *Science* **2019**, *366*, 1209–1211.

[119] Filleter, T.; McChesney, J. L.; Bostwick, A.; Rotenberg, E.; Emtsev, K. V.; Seyller, T.; Horn, K.; Bennewitz, R. Friction and dissipation in epitaxial graphene films. *Phys. Rev. Lett.* **2009**, *102*, 086102.

[120] Sohier, T.; Calandra, M.; Mauri, F. Density functional perturbation theory for gated two-dimensional heterostructures: Theoretical developments and application to flexural phonons in graphene. *Phys. Rev. B* **2017**, *96*, 075448.

[121] Huang, G. W.; Wang, R. C.; Wu, W. C.; Xue, W. L.; Wang, P.; Li, H. L.; Gong, Z. B. Investigating the current-carrying friction mechanism of n-type and p-type two-dimensional TMD under a positive electric field. *ACS Appl. Mater. Interfaces* **2025**, *17*, 4107–4113.

[122] Qu, C. Y.; Wang, K. Q.; Wang, J.; Gongyang, Y. J.; Carpick, R. W.; Urbakh, M.; Zheng, Q. S. Origin of friction in superlubric graphite contacts. *Phys. Rev. Lett.* **2020**, *125*, 126102.

[123] Peng, D. L.; Wu, Z. H.; Shi, D. W.; Qu, C. Y.; Jiang, H. Y.; Song, Y. M.; Ma, M.; Aeppli, G.; Urbakh, M.; Zheng, Q. S. Load-induced dynamical transitions at graphene interfaces. *Proc. Natl. Acad. Sci. USA* **2020**, *117*, 12618–12623.

[124] Liu, Y. M.; Wang, K.; Xu, Q.; Zhang, J.; Hu, Y. Z.; Ma, T. B.; Zheng, Q. S.; Luo, J. B. Superlubricity between graphite layers in ultrahigh vacuum. *ACS Appl. Mater. Interfaces* **2020**, *12*, 43167–43172.

[125] Bruch, L. W. Ohmic damping of center-of-mass oscillations of a molecular monolayer. *Phys. Rev. B* **2000**, *61*, 16201–16206.

[126] Hu, H. Q.; Xia, K. L.; Zhao, S. J.; Ma, M.; Zheng, Q. S. Eliminating graphene wrinkles by strain engineering. *Extrem. Mech. Lett.* **2021**, *42*, 101104.

[127] Zhao, S. J.; Shi, S. L.; Xia, K. L.; Wang, T.; Chai, M. S.; Zhang, Y. Y.; Qu, C. Y.; Zheng, Q. S. Scratching of graphene-coated Cu substrates leads to hardened Cu interfaces with enhanced lubricity. *ACS Appl. Nano Mater.* **2020**, *3*, 1992–1998.

[128] Huang, X. Y.; Lin, L.; Zheng, Q. S. Theoretical study of superlubric nanogenerators with superb performances. *Nano Energy* **2020**, *70*, 104494.

[129] Zhao, S. J.; Zhang, Z. H.; Wu, Z. H.; Liu, K. H.; Zheng, Q. S.; Ma, M. The impacts of adhesion on the wear property of graphene. *Adv. Mater. Interfaces* **2019**, *6*, 1900721.

[130] Zhang, Y. F.; Li, B.; Zheng, Q. S.; Genin, G. M.; Chen, C. Q. Programmable and robust static topological solitons in mechanical metamaterials. *Nat. Commun.* **2019**, *10*, 5605.

[131] Huang, S. Y.; Wei, Z. Y.; Duan, Z. Q.; Sun, C. D.; Wang, Y. K.; Tao, Y.; Zhang, Y.; Kan, Y. J.; Meyer, E.; Li, D. Y. et al. Reexamination of damping in sliding friction. *Phys. Rev. Lett.* **2024**, *132*, 056203.

[132] Wu, S.; He, Y. Q.; Zheng, Q. S.; Ma, M. Oscillating friction of nanoscale capillary bridge. *Friction* **2022**, *10*, 200–208.

[133] Huang, X. Y.; Xiang, X. J.; Nie, J. H.; Peng, D. L.; Yang, F. W.; Wu, Z. H.; Jiang, H. Y.; Xu, Z. P.; Zheng, Q. S. Microscale Schottky superlubric generator with high direct-current density and ultralong life. *Nat. Commun.* **2021**, *12*, 2268.

[134] Wang, K. Q.; Qu, C. Y.; Wang, J.; Quan, B. G.; Zheng, Q. S. Characterization of a microscale superlubric graphite interface. *Phys. Rev. Lett.* **2020**, *125*, 026101.

[135] Song, A. S.; Gao, L.; Zhang, J.; Liu, X.; Hu, Y. Z.; Ma, T. B.; Zheng, Q. S.; Luo, J. B. Achieving a superlubricating ohmic sliding electrical contact via a 2D heterointerface: A computational investigation. *Nanoscale* **2020**, *12*, 7857–7863.

[136] Wang, P.; Su, B. Q.; Gao, X. C.; Yan, W. S.; Wang, R. C.; Xue, W. L.; Li, H. L.; Wang, N.; Gong, Z. B. Voltage regulation of atomic-scale energy dissipation at niobium diselenide electro-friction interface. *Tribol. Int.* **2025**, *204*, 110534.

[137] Kwon, S.; Ko, J. H.; Jeon, K. J.; Kim, Y. H.; Park, J. Y. Enhanced nanoscale friction on fluorinated graphene. *Nano Lett.* **2012**, *12*, 6043–6048.

[138] Li, Q. Y.; Liu, X. Z.; Kim, S. P.; Shenoy, V. B.; Sheehan, P. E.; Robinson, J. T.; Carpick, R. W. Fluorination of graphene enhances friction due to increased corrugation. *Nano Lett.* **2014**, *14*, 5212–5217.

[139] Deng, Z.; Smolyanitsky, A.; Li, Q. Y.; Feng, X. Q.; Cannara, R. J. Adhesion-dependent negative friction coefficient on chemically modified graphite at the nanoscale. *Nat. Mater.* **2012**, *11*, 1032–1037.

[140] Lang, H. J.; Peng, Y. T.; Zeng, X. Z.; Cao, X. A.; Liu, L.; Zou, K. Effect of relative humidity on the frictional properties of graphene at atomic-scale steps. *Carbon* **2018**, *137*, 519–526.

[141] Lang, H. J.; Peng, Y. T.; Shao, G. W.; Zou, K.; Tao, G. M. Dual control of the nanofriction of graphene. *J. Mater. Chem. C* **2019**, *7*, 6041–6051.

[142] Zhang, Y. X.; Peng, Y. T.; Lang, H. J.; Huang, Y.; Cao, X. A. Electric-carrying nanofriction properties of atomic-scale steps on graphene. *Tribol. Lett.* **2020**, *68*, 121.

[143] Tang, Q.; Huang, Y. H.; Sun, D. E.; Li, Q. Y. Effect of humidity on the wear behavior of graphene under current carrying conditions. *Tribol. Lett.* **2025**, *73*, 8.

[144] Zhao, S. Q.; Luo, P.; Yang, S. J.; Zhou, X.; Wang, Z. M.; Li, C. L.; Wang, S. P.; Zhai, T. Y.; Tao, X. T. Low-symmetry and nontoxic 2D SiP with strong polarization-sensitivity and fast photodetection. *Adv. Opt. Mater.* **2021**, *9*, 2100198.

[145] Lang, H. J.; Zou, K.; Chen, R. L.; Huang, Y.; Peng, Y. T. Role of interfacial water in the tribological behavior of graphene in an electric field. *Nano Lett.* **2022**, *22*, 6055–6061.

[146] Sekhar, M. C.; Veena, E.; Kumar, N. S.; Naidu, K. C. B.; Mallikarjuna, A.; Basha, D. B. A review on piezoelectric materials and their applications. *Cryst. Res. Technol.* **2023**, *58*, 2200130.

[147] Dong, H. W.; Zhu, Z. Y.; Li, Z.; Li, M. M.; Chen, J. Y. Piezoelectric composites: State-of-the-art and future prospects. *JOM* **2024**, *76*, 340–352.

[148] Wang, L.; Zhang, D. W.; Luo, Z. D.; Sharma, P.; Seidel, J. Inhomogeneous friction behaviour of nanoscale phase separated layered $CuInP_2S_6$. *Adv. Funct. Mater.* **2023**, *33*, 2303583.
[149] Wang, K. Q.; Ouyang, W. E.; Cao, W.; Ma, M.; Zheng, Q. S. Robust superlubricity by strain engineering. *Nanoscale* **2019**, *11*, 2186–2193.
[150] Wang, J.; Cao, W.; Song, Y. M.; Qu, C. Y.; Zheng, Q. S.; Ma, M. Generalized scaling law of structural superlubricity. *Nano Lett.* **2019**, *19*, 7735–7741.
[151] Sun, T. T.; Wu, Z. H.; Li, Z. H.; Zheng, Q. S.; Lin, L. A hybrid two-axis force sensor for the mesoscopic structural superlubricity studies. *Sensors* **2019**, *19*, 3431.
[152] Qu, C. Y.; Shi, S. L.; Ma, M.; Zheng, Q. S. Rotational instability in superlubric joints. *Phys. Rev. Lett.* **2019**, *122*, 246101.
[153] Socoliuc, A.; Gnecco, E.; Maier, S.; Pfeiffer, O.; Baratoff, A.; Bennewitz, R.; Meyer, E. Atomic-scale control of friction by actuation of nanometer-sized contacts. *Science* **2006**, *313*, 207–210.
[154] Liu, Z.; Yang, H.; Wang, S.; Wu, J. X.; Ouyang, W. G.; Zhang, J. Y.; Luo, F. Energy dispersion induced precisely tunable friction of graphitic interface. *Adv. Sci.* **2025**, *12*, 2500378.
[155] Peng, Y. T.; Hu, Y. Z.; Wang, H. Tribological behaviors of surfactant-functionalized carbon nanotubes as lubricant additive in water. *Tribol. Lett.* **2007**, *25*, 247–253.
[156] Peng, Y. T.; Huang, D. Fabrication of patterned reduced graphene oxide nanosheet field-emission cathodic film at room-temperature. *Appl. Surf. Sci.* **2013**, *283*, 81–86.
[157] Peng, Y. T.; Ni, Z. H. Tribological properties of stearic acid modified multi-walled carbon nanotubes in water. *J. Tribol.* **2013**, *135*, 012001.
[158] Liu, J.; Qi, Y. Z.; Li, Q. Y.; Duan, T. Y.; Yue, W.; Vadakkepatt, A.; Ye, C.; Dong, Y. L. Vacancy-controlled friction on 2D materials: Roughness, flexibility, and chemical reactions. *Carbon* **2019**, *142*, 363–372.
[159] Zhang, X. S.; Xu, P. P.; Hou, T. H.; Lang, H. J.; Peng, Y. T. Ultra-low friction of flexoelectric bubble on atomically thin suspended h-BN. *Nano Energy* **2024**, *126*, 109614.
[160] Peng, Y. T.; Deng, K. Fabrication of reduced graphene oxide nanosheets reinforced Sn-Bi nanocomposites by electro-chemical deposition. *Compos. Part A: Appl. Sci. Manuf.* **2015**, *73*, 55–62.
[161] Peng, Y. T.; Deng, K. Study on the mechanical properties of the novel Sn-Bi/graphene nanocomposite by finite element simulation. *J. Alloys Compd.* **2015**, *625*, 44–51.
[162] He, X. J.; Yu, T. T.; Wu, Z. S.; Du, C. H.; Deng, H. Y.; Zhao, Y. K.; Li, S.; Feng, Y. G.; Zhang, L. Q.; Zhang, Z. N. et al. Atomically thin MoS_2 with ultra-low friction properties based on strong interface interaction. *Friction* **2025**, *13*, 9440936.
[163] Deng, H. Y.; Yu, T. T.; Du, C. H.; Shen, R. L.; Zhao, Y. K.; He, X. J.; Feng, Y. G.; Zhang, L. Q.; Wang, D. A. Nickel phosphorous trisulfide: A ternary 2D material with an ultra-low coefficient of friction. *Friction* **2024**, *12*, 2313–2324.
[164] Deng, H. Y.; Yu, T. T.; He, X. J.; Li, S.; Du, C. H.; Liu, P. F.; Shen, R. L.; Feng, Y. G.; Zhang, L. Q.; Wang, D. A. Gas modulation induced ultra-low friction and ultra-strong wear resistance in atomically thin $MoSe_2$ single crystals. *Small* **2025**, *21*, e08227.
[165] Wang, Y.; Cheng, Y.; Wang, Y. L.; Zhang, S.; Xu, C.; Zhang, X. W.; Wang, M.; Xia, Y.; Li, Q. Y.; Zhao, P. et al. Chemical vapor deposition growth of graphene domains across the Cu grain boundaries. *Nano* **2018**, *13*, 1850088.
[166] Zhang, S.; Gao, L.; Song, A. S.; Zheng, X. H.; Yao, Q. Z.; Ma, T. B.; Di, Z. F.; Feng, X. Q.; Li, Q. Y. Tuning local electrical conductivity via fine atomic scale structures of two-dimensional interfaces. *Nano Lett.* **2018**, *18*, 6030–6036.
[167] Dai, Z. H.; Wang, G. R.; Zheng, Z. Y.; Wang, Y. L.; Zhang, S.; Qi, X. Y.; Tan, P. H.; Liu, L. Q.; Xu, Z. P.; Li, Q. Y. et al. Mechanical responses of boron-doped monolayer graphene. *Carbon* **2019**, *147*, 594–601.
[168] Zeng, X. Z.; Peng, Y. T.; Liu, L.; Lang, H. J.; Cao, X. A. Dependence of the friction strengthening of graphene on velocity. *Nanoscale* **2018**, *10*, 1855–1864.
[169] Zeng, X. Z.; Peng, Y. T.; Yu, M. C.; Lang, H. J.; Cao, X. A.; Zou, K. Dynamic sliding enhancement on the friction and adhesion of graphene, graphene oxide, and fluorinated graphene. *ACS Appl. Mater. Interfaces* **2018**, *10*, 8214–8224.
[170] Cao, X. A.; Gan, X. H.; Lang, H. J.; Yu, K.; Ding, S. Y.; Peng, Y. T.; Yi, W. M. Anisotropic nanofriction on MoS_2 with different thicknesses. *Tribol. Int.* **2019**, *134*, 308–316.
[171] Yao, Q. Z.; Qi, Y. Z.; Zhang, J.; Zhang, S.; Zhao, P.; Wang, H. T.; Feng, X. Q.; Li, Q. Y. Impacts of the substrate stiffness on the anti-wear performance of graphene. *AIP Adv.* **2019**, *9*, 075317.
[172] Yuan, W. F.; Yao, Y.; Keer, L.; Jiao, Y. W.; Yu, J. X.; Li, Q. Y.; Feng, X. Q. 3D-printed biomimetic surface structures with abnormal friction properties. *Extrem. Mech. Lett.* **2019**, *26*, 46–52.
[173] Peng, Y. T.; Hu, Y. R.; Han, L. Z.; Ren, C. X. Ultrasound-assisted fabrication of dispersed two-dimensional copper/reduced graphene oxide nanosheets nanocomposites. *Compos. Part B: Eng.* **2014**, *58*, 473–477.
[174] Peng, Y. T.; Wang, Z. Q. Tribological properties of sodium dodecyl sulfate aqueous dispersion of graphite-derived carbon materials. *RSC Adv.* **2014**, *4*, 9980–9985.
[175] Peng, Y. T.; Wang, Z. Q.; Li, C. Study of nanotribological properties of multilayer graphene by calibrated atomic force microscopy. *Nanotechnology* **2014**, *25*, 305701.
[176] Sun, M. L.; Peng, Y. T. Study on structural, electronic and magnetic properties of Sn atom adsorbed on defective graphene by first-principle calculations. *Appl. Surf. Sci.* **2014**, *307*, 158–164.
[177] Peng, Y. T.; Wang, Z. Q.; Zou, K. Friction and wear properties of different types of graphene nanosheets as effective solid lubricants. *Langmuir* **2015**, *31*, 7782–7791.
[178] Peng, Y. T.; Ye, J. X.; Zheng, L. L.; Zou, K. The hydrogen sensing properties of Pt-Pd/reduced graphene oxide based sensor under different operating conditions. *RSC Adv.* **2016**, *6*, 24880–24888.
[179] Lang, H. J.; Peng, Y. T.; Zeng, X. Z. Effect of interlayer bonding strength and bending stiffness on 2-dimensional materials' frictional properties at atomic-scale steps. *Appl. Surf. Sci.* **2017**, *411*, 261–270.
[180] Liu, L.; Huang, Z. B.; Peng, Y. T.; Huang, P. Enhanced lubrication and photocatalytic degradation of liquid paraffin by coral-like MoS_2. *New J. Chem.* **2017**, *41*, 7674–7680.
[181] Sulollari, E.; van Dalen, K. N.; Cabboi, A. Vibration-induced friction modulation for a general frequency of excitation. *J. Sound Vibr.* **2024**, *573*, 118200.
[182] Liu, J. X.; Yang, X. Q.; Fang, H.; Yan, W. D.; Ouyang, W. G.; Liu, Z. *In situ* twistronics: A new platform based on superlubricity. *Adv. Mater.* **2025**, *37*, 2305072
[183] Peng, Y. T.; Zeng, X. Z.; Liu, L.; Cao, X. G.; Zou, K.; Chen, R. L. Nanotribological characterization of graphene on soft elastic substrate. *Carbon* **2017**, *124*, 541–546.
[184] Peng, Y. T.; Zheng, L. L.; Zou, K.; Li, C. Enhancing performances of a resistivity-type hydrogen sensor based on $Pd/SnO_2/RGO$ nanocomposites. *Nanotechnology* **2017**, *28*, 215501.
[185] Zeng, X. Z.; Peng, Y. T.; Lang, H. J. A novel approach to decrease friction of graphene. *Carbon* **2017**, *118*, 233–240.
[186] Huang, Y. H.; Li, Q. Y.; Zhang, J.; Qi, Y. Z.; Wang, H. T.; Zhao, P.; Meng, Y. G. Effect of airborne contaminants on the macroscopic anti-wear performance of chemical vapor deposition graphene. *Surf. Coat. Technol.* **2020**, *383*, 125276.
[187] Meng, L.; Li, Y.; Liu, T. S.; Zhu, C. Y.; Li, Q. Y.; Chen, X. J.; Zhang, S.; Zhang, X.; Bao, L. H.; Huang, Y. et al. Wrinkle networks

in exfoliated multilayer graphene and other layered materials. *Carbon* **2020**, *156*, 24–30.
[188] Zhu, R. J.; Wang, Z. M.; Yao, Q. Z.; Li, Q. Y.; Cheng, Z. X.; Guo, X. L.; Zhang, T.; Li, X. S.; Kimura, H.; Matsumoto, T. et al. Thickness-dependent frictional behavior of topological insulator Bi_2Se_3 nanoplates. *Appl. Phys. A* **2020**, *126*, 285.
[189] Zeng, X. Z.; Peng, Y. T.; Lang, H. J.; Cao, X. A. Nanotribological behavior of a single silver nanowire on graphite. *Nanotechnology* **2018**, *29*, 085706.
[190] Zeng, X. Z.; Peng, Y. T.; Lang, H. J.; Yu, K. Probing the difference in friction performance between graphene and MoS_2 by manipulating the silver nanowires. *J. Mater. Sci.* **2019**, *54*, 540–551.
[191] Zeng, X. Z.; Peng, Y. T.; Lang, H. J.; Liu, L. Controllable nanotribological properties of graphene nanosheets. *Sci. Rep.* **2017**, *7*, 41891.
[192] Cao, X. A.; Gan, X. H.; Peng, Y. T.; Wang, Y. X.; Zeng, X. H.; Lang, H. J.; Deng, J. N.; Zou, K. An ultra-low frictional interface combining FDTS SAMs with molybdenum disulfide. *Nanoscale* **2018**, *10*, 378–385.
[193] Liu, L.; Jiao, S. L.; Peng, Y. T.; Zhou, W. A green design for lubrication: Multifunctional system containing Fe_3O_4@MoS_2 nanohybrid. *ACS Sustain. Chem. Eng.* **2018**, *6*, 7372–7379.
[194] Li, S.; Yu, T. T.; Du, C. H.; Deng, H. Y.; He, X. J.; Zhao, Y. K.; Feng, Y. G.; Zhang, L. Q.; Wang, Y. Q.; Wang, D. A. Large scale and ultra-thin conductive two-dimensional metal films (< 3.5 nm) for fast flexible electronics. *Mater. Today* **2025**, *86*, 52–62.
[195] Wei, Z. Y.; Han, D.; Wang, Q.; Sun, C. D.; Tao, Y.; Xiang, L.; Kan, Y. J.; Zhang, Y.; Lu, X.; Chen, Y. F. Modulating friction by the phase of the vertical vibrational excitation at washboard frequency. *ACS Appl. Mater. Interfaces* **2023**, *15*, 45516–45525.
[196] Wang, Y. X.; Cao, X. A.; Lang, H. J.; Zeng, X. Z.; Chen, B.; Chen, R. L.; Peng, Y. T. Enhanced tribological properties of composite films based on ionic liquids with MoS_2 nanosheets as additives. *New J. Chem.* **2018**, *42*, 4887–4892.
[197] Zeng, X. Z.; Peng, Y. T.; Lang, H. J.; Cao, X. A. Tuning the nanotribological behaviors of single silver nanowire through various manipulations. *Appl. Surf. Sci.* **2018**, *440*, 830–840.